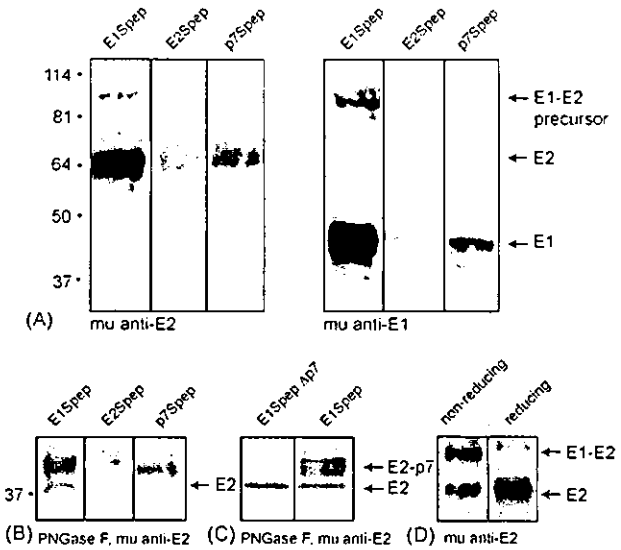

Fig. 3. Characterization of Spep-tagged HCV envelope glycoproteins. Expressed proteins were precipitated using S-protein agarose (SAG) and Western blots were visualized using murine MAbs directed to either E1 (MAbs #299 and #384) or E2 (MAbs #187) as indicated below the image (mu anti-E1 or mu anti-E2, respectively). Molecular weight markers are indicted at left. (A) Isolation by SAG precipitation of E2 (left) and E1 (right) from cells expressing E1Spep, E2Spep and p7Spep. The mature E1 and E2 glycoproteins are indicated at right; residual unprocessed E1–E2 precursor is also visible. (B) Isolated glycoproteins were deglycosylated using PNGase F and E2-reactive polypeptides were detected using murine anti-E2 MAb. The expected position of the E2 polypeptide is indicated. (C) p7 Expression was ablated from the E1Spep polyprotein by introducing a stop codon at the E2–p7 junction (E1SpepΔp7). Glycoproteins were deglycosylated using PNGase F and E2 polypeptides were detected using murine anti-E2 MAb. E2 and E2–p7 polypeptides are indicated. (D) The E1–E2 complex from E1Spep polyprotein was isolated and resolved by SDS-PAGE under non-reducing or reducing conditions. The E2 glycoprotein and the disulfide-crosslinked E1–E2 complex are indicated.

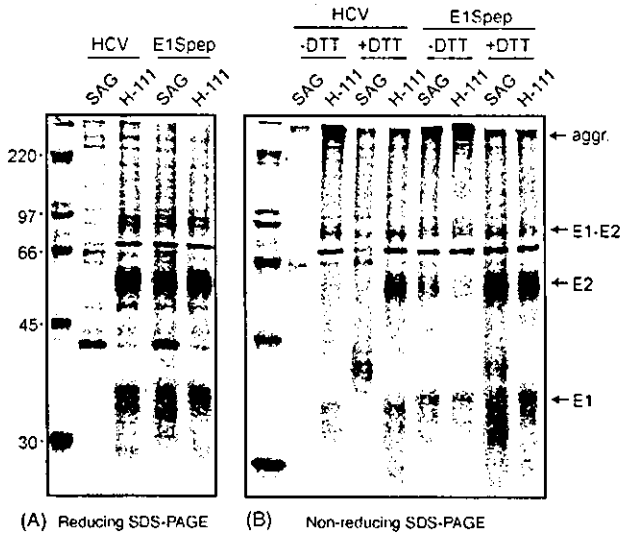

Fig. 4. Isolation of noncovalently associated E1–E2 complex under mildly reducing conditions. Cells expressing the untagged HCV structural polyprotein or the E1Spep polyprotein were metabolically labeled using ^{35}S-methionine and -cysteine and lysed in solubilization buffer with (+DTT) or without (−DTT) 1 mM DTT. E1–E2 complexes were precipitated using either SAG or a human anti-E1 MAb H-111. Isolated proteins were resolved by SDS-PAGE under reducing (A) or non-reducing (B) conditions. Free E1 and E2 are indicated, as are the covalently linked E1–E2 complex/precursor (E1–E2) and the higher molecular weight aggregates (aggr.). Cells expressing the untagged HCV polyprotein served as control for the SAG precipitation. ^{14}C-labeled molecular weight markers (Amersham Biosciences) are shown at left. The identity of the additional bands (≈ 40 and 70 kDa) is unknown.

under nonreducing conditions. In these experiments, the misfolded disulfide-crosslinked E1–E2 complex migrates slowly, whereas the noncovalently associated E2 migrates as the free glycoprotein. From these studies (Fig. 3D), we estimated that ≈25% of the E2 glycoprotein isolated by using the E1Spep tag was in the form of noncovalently associated complex. Although this percentage is similar to that reported for the untagged HCV polyproteins (Deleersnyder et al., 1997; Dubuisson et al., 1994; Dubuisson and Rice, 1996 and see below), we were surprised at the extent of apparent misfolding.

In order to investigate the source of the disulfide-crosslinked aggregates commonly found upon expression of the HCV envelope glycoproteins, we modified our cell lysis buffer to include 1 mM DTT. We reasoned that this low level of reducing agent might mitigate against the oxidative environment in the ER (Tatu et al., 1993) but would itself be unable to reduce properly folded protein. If proper folding of the expressed glycoproteins were limited kinetically, then this low level of reducing agent might enhance the isolation of properly folded, noncovalently associated complex. We explored this hypothesis using both the native, untagged HCV structural polyprotein and the affinity-tagged E1Spep polyprotein. Cells were metabolically labeled and lysed in the presence or absence of 1 mM DTT. Complexes were then immunoprecipitated using either SAG, or a human anti-E1 MAb H-111 (Z.-Y. Keck and S.K.H. Foung; unpublished). Overall yields were similar in the presence or absence of DTT and lysis in the presence of 1 mM DTT did not disrupt the E1–E2 association (Fig. 4A). As analyzed by SDS-PAGE under reducing conditions, comparable amounts of E1–E2 complex were isolated by H-111 from cells expressing the tagged or untagged HCV polyprotein, suggesting retention of the MAb epitope. Importantly, both tagged and untagged complexes isolated in the presence of 1 mM DTT were largely noncovalently associated (Fig. 4B). By contrast, samples prepared in the absence of 1 mM DTT showed significant amounts of E1–E2 aggregation, and commensurately lesser amounts of noncovalently associated E1 and E2.

We speculate that lysis under mildly reducing conditions may prevent artefactual disulfide bond formation during isolation or, more likely, may facilitate disulfide bond reshuffling in the nascent complex. We presume that, in the absence of competing and irreversible disulfide bond formation, the glycoprotein complex in the presence of 1 mM DTT is able to fold into its native state.

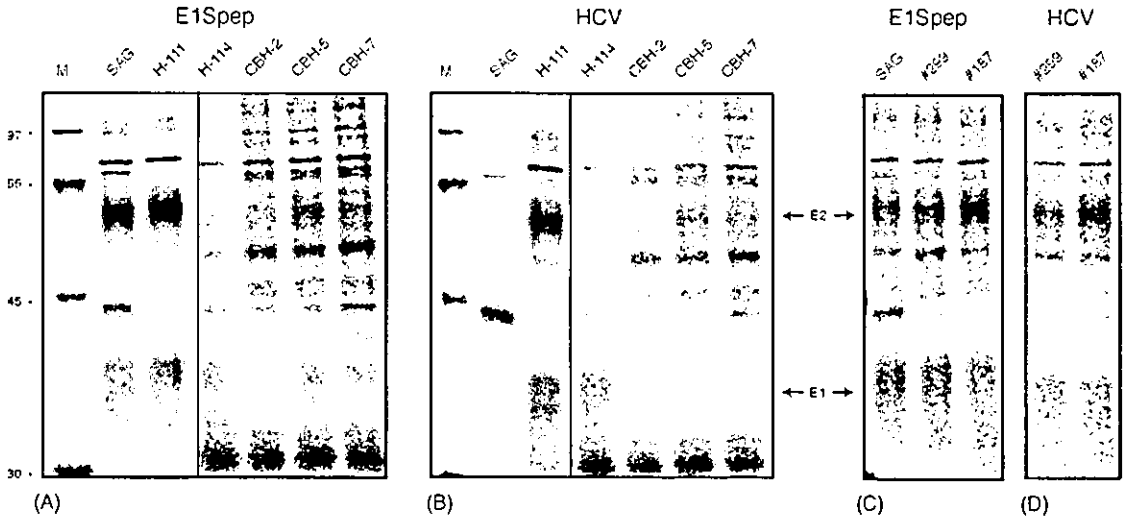

Fig. 5. Immunoprecipitation of E1–E2 complexes. Cells expressing the E1Spep (panels A and C) or the untagged HCV (panels B and D) polyprotein were metabolically labeled and lysed in solubilization buffer containing 1 mM DTT. Complexes were precipitated using the indicated reagents: SAG, human anti-E1 MAbs H-111 or H-114, human anti-E2 MAbs CBH-2, CBH-5 or CBH-7, or with murine anti-E1 MAb #299 or murine anti-E2 MAb #187. (A) Isolation of E1Spep-E2 complex using human MAbs. The image representing SAG and H-111 has been significantly lightened relative to that of the other human MAbs. Quantitation of radioactivity revealed that, relative to H-111, CBH-2 was able to precipitate 2% of the E2 glycoprotein, CBH-5 (13%), and CBH-7 (11%). Significant amounts were not detected using H-114. (B) Isolation of E1–E2 complex from untagged HCV polyprotein. Lanes representing SAG and H-111 are significantly lightened. Relative yields of E2 glycoprotein for CBH-5 and CBH-7 were 6 and 5%, respectively; no significant amounts of E2 were detected using H-114 or CBH-2. (C) and (D) Isolation of, respectively, E1Spep and HCV complex using murine MAbs #299 and #187.

3.3. Monoclonal antibodies as structural probes

To further assess the structural integrity of the noncovalently associated complex, we examined the ability of MAbs to recognize the solubilized glycoproteins. As depicted in Fig. 5, E1–E2 complex from cells expressing either the tagged or untagged HCV structural polyproteins was readily immunoprecipitated by murine MAbs directed against linear epitopes in either E1 or E2 (#299 and #187, respectively) and by the human anti-E1 MAb H-111. A significantly lesser amount of E1–E2 complex was isolated using conformation-dependent human MAbs directed to E1 (MAb H-114; Z.-Y. Keck and S.K.H. Foung, unpublished) or E2 (MAbs CBH-2, CBH-5 and CBH-7 (Hadlock et al., 2000; Triyatni et al., 2002)). Although these anti-E2 MAbs were isolated from a patient infected with a genotype 1b virus (Hadlock et al., 2000), we were able to recover at most 13% of the E1–E2 complex of this genotype 1b isolate. In other experiments, a similar pattern of reactivity was observed using complexes prepared in the absence of 1 mM DTT (data not shown). The overall diminution in reactivity of these human MAbs may be ascribed to antigenic differences between the virus of the MAb donor and those represented in the expression plasmid, or to conformational differences in the isolated complex. Importantly, however, the pattern of MAb reactivity was identical using complexes derived from the tagged and untagged HCV polyprotein. These parallels suggest that the immunochemical structure of the complex was not grossly perturbed by the introduction of the affinity tag.

Further attempts to ascertain the integrity of the complexes using a soluble form of the putative HCV receptor CD81 (Flint et al., 1999) were uninformative in that CD81 does not bind to genotype 1b glycoproteins (Roccasecca et al., 2003; Triyatni et al., 2002; Yagnik et al., 2000).

3.4. MAb binding to affinity-captured E1Spep–E2 complex and proteoliposomes

Taken together, our analyses suggested that assembly of the E1–E2 complex was largely unaffected by the introduction of the affinity tag at position 295/296 in E1. Based on computer predictions that the E1 glycoprotein may be able to adopt a polytopic topology in which the Spep-tagged region would lie on the cytoplasmic side of the membrane, we sought to reconstruct the predicted topology of the E1Spep glycoprotein by generating affinity-captured and properly oriented proteoliposomal complexes. We first used S-protein-conjugated paramagnetic beads to isolate E1Spep–E2 complex. Bound E1Spep was readily detected by flow cytometry using murine anti-E1 MAbs or the human MAbs H-111 (Fig. 6A) and associated E2 glycoprotein was demonstrated by Western blot analysis using the anti-E2 MAb #187 (Fig. 6B). The nonionic detergent was then replaced with a liposomal membrane to examine membrane topology. Because lipid accretion occurs at transmembrane regions of the bound proteins, continued exposure of E1 and E2 epitopes upon reconstitution would suggest that the ectodomains of E1 and E2 are properly oriented in the proteoliposome, despite anchoring by the affinity tag.

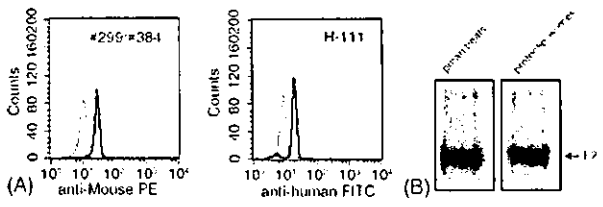

Fig. 6. Analysis of E1Spep and E2 glycoproteins on paramagnetic beads and proteoliposomes. S-protein coupled Dynabeads were used to isolate E1–E2 complex from lysates of cells expressing the E1Spep polyprotein. (A) Flow cytometric analysis of paramagnetic beads. Beads were incubated with anti-E1 MAbs in buffer containing 0.5% Cymal-5 nonionic detergent. Murine MAbs #299 and #384 (pooled) were detected using a second antibody labeled with phycoerythrin (PE); human MAb H-111 was detected using a second antibody labeled with fluorescein isothiocyanate (FITC). Histograms are shown in black lines. The negative control (filled, gray histograms) for the murine MAbs are paramagnetic beads bearing Spep-tagged CD4 (Gallina et al., 2002) and stained using the murine anti-E1 MAbs; the negative control for the human MAb are E1Spep paramagnetic beads stained using the anti-HIV MAb 447-52D (Conley et al., 1994). (B) Western blot analysis of E2 glycoprotein captured via E1Spep on paramagnetic beads (pmag beads) and subsequently retained in proteoliposomes. Lysates were prepared in solubilization buffer containing 1 mM DTT and bound E2 glycoprotein was detected using non-reducing SDS-PAGE and murine anti-E2 MAb #187.

Using protocols derived from Sodroski and colleagues (Babcock et al., 2001; Grundner et al., 2002; Mirzabekov et al., 2000), a mixture of synthetic lipids was added to the suspension of paramagnetic beads bearing the E1Spep–E2 complex, and the Cymal-5 nonionic detergent was then removed by dialysis to allow formation of the proteoliposomal membrane. Lipid accretion was sufficient to cover the paramagnetic bead, albeit not necessarily as a continuous membrane (see Section 2), and biochemical analysis of the reconstituted E1Spep–E2 proteoliposomes showed complete retention of the noncovalently associated E2 glycoprotein (Fig. 6B). Proteoliposomes constructed in this manner have, in many cases, been shown to display properly oriented and correctly folded glycoproteins (Grundner et al., 2002; Mirzabekov et al., 2000; Rigaud et al., 1995; Walter et al., 1990; CTM and JHN, unpublished).

Murine and human MAbs that recognized the detergent-solubilized E1Spep–E2 complex also recognized the proteoliposomal complex (Fig. 7). Linear epitopes within the E1 glycoprotein remained accessible to binding by murine MAbs #299 and #384, and #159 (kindly provided by J. Lau; (Triyatni et al., 2002)) and by the human anti-E1 MAb H-111. The retention of E1 glycoprotein exposure and reactivity, despite saturating amounts of lipid, is consistent with formation of the lipid bilayer between the ectodomain and the Spep anchor on the bead. Accretion of even a discontinuous bilayer at a single, C-terminal transmembrane domain would be anticipated to occlude antibody access to the now-buried ectodomain. In fact, binding to the proteoliposomes was comparable to that seen with the same paramagnetic beads prior to membrane accretion (see Fig. 6). The proteoliposomal E2 glycoprotein also remained accessible to murine MAb #187. As anticipated, little or no binding was detected using human MAbs that only weakly recognized the solubilized complexes (H-114, CBH-2, CBH-5 and CBH-7; Fig. 7).

Taken together, these studies suggest that the immunochemical properties of the E1Spep–E2 complex were unchanged by membrane reconstitution. These results are consistent with the prediction that E1 glycoprotein can assume a polytopic topology consisting of two membrane-spanning domains — the internal and C-terminal transmembrane regions — and an intervening cytoplasmic loop. In our studies with proteoliposomes, this topology was enforced by the Spep affinity tag. The parallel immune reactivity of the tagged and untagged glycoproteins in solution, however, suggests that the E1 glycoprotein may naturally display flexibility in its folding and membrane topology.

4. Discussion

Our studies suggest that the HCV E1 glycoprotein is able to adopt a polytopic topology in which the heterodimeric noncovalent association with the E2 glycoprotein subunit is retained. Further studies are clearly needed to prove the existence of this alternative form, and to define its relationship to the canonical, Type I form of the E1 glycoprotein. In the absence of a productive cell culture system for the growth of infectious HCV, direct links between envelope glycoprotein structure and function are difficult to demonstrate. In fact, a firm definition of the native structure(s) of the HCV envelope glycoproteins remains elusive despite the recent development of infectious pseudotyped virions bearing the E1–E2 complex (Bartosch et al., 2003; Drummer et al., 2003; Hsu et al., 2003). Nonetheless, our studies highlight the possibility that the E1 glycoprotein is capable of topologic flexibility.

In considering a cytoplasmic loop in the E1 glycoprotein (amino acids 285–344), it is perhaps significant that the potential glycosylation site at amino acid 325 is not utilized in the wild-type E1 glycoprotein (Meunier et al., 1999). Mutation to a more optimal glycosylation motif (NWSP to NTSG) enables only partial utilization of this site (Meunier et al., 1999). It is unclear whether the unglycosylated fraction reflects suboptimal glycosylation or a mixture of E1 topologies. Similarly, although the glycosylation site at position 305 appears to be utilized in some E1 glycoproteins (Meunier et al., 1999), this position is variably glycosylated in the genotype 1b isolate used here (YM, unpublished).

Topologic flexibility during biogenesis has been reported for other viral envelope glycoproteins. In the case of Hepatitis B virus, the surface glycoprotein is initially formed in the ER with the entire pre-S domain located in the cytosol; during maturation, 50% of the glycoprotein is converted to an alternative topology wherein the pre-S domain is translocated through the membrane to the lumenal side (Lambert and Prange, 2001 and references therein). Recently, Morri-

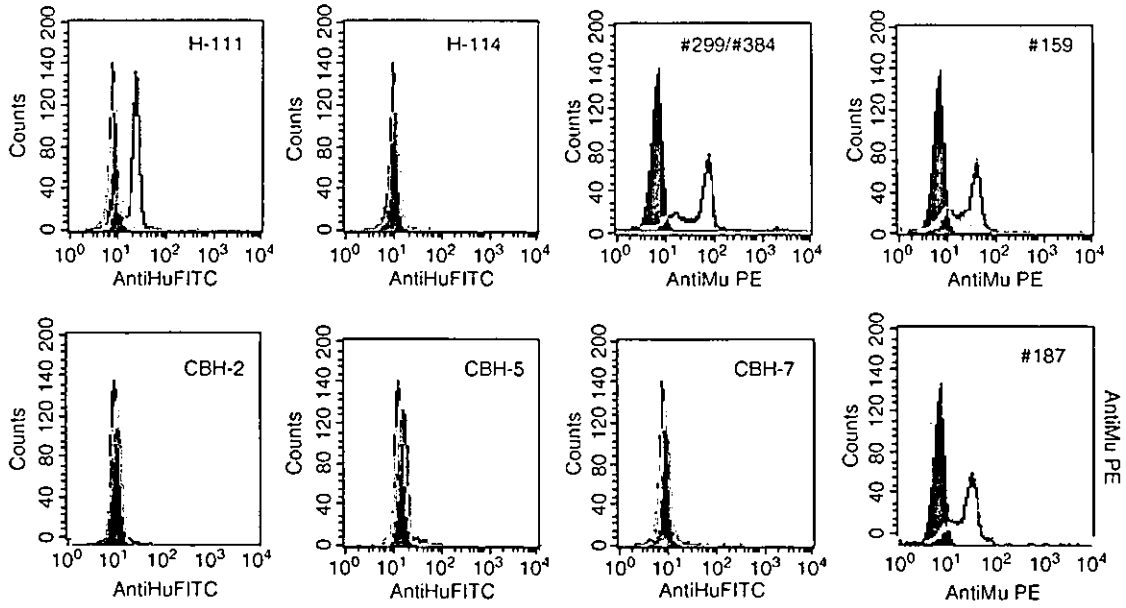

Fig. 7. Flow cytometric analysis of MAb binding to proteoliposomal E1–E2 complexes. Proteoliposomal beads were incubated with the indicated human or murine MAbs and subsequently stained using the appropriate secondary antibody conjugated, respectively, to FITC or PE. The murine anti-E1 MAb #159 was kindly provided by J. Lau (Triyatni et al., 2002). Control human MAbs directed to irrelevant antigens (HIV envelope glycoprotein gp120 and gp41, respectively) were kindly provided by S. Zolla-Pazner and M. Posner. A murine anti-gp41 MAb served as negative control for the murine anti-HCV MAbs and was kindly provided by G. Lewis. Histograms of anti-HCV MAb binding are shown by gray lines; control anti-HIV MAbs are shown in solid black histograms. For MAb H-111, the absence of binding to HIV-1 gp160 proteoliposomal beads (unpublished) is indicated in gray within the negative peak. The source of the minor, dull peak seen using the murine anti-HCV MAbs is unclear.

son and colleagues have reported that the fusion glycoprotein of Newcastle disease virus (NDV), for which a Type I membrane topology is well documented, can also assume a polytopic topology (McGinnes et al., 2003). The specific polytopic topology of the NDV fusion glycoprotein is similar to that which we propose for the HCV E1 glycoprotein.

If a cytoplasmic loop of E1 is involved in interactions with the virion core, as has been suggested (Lo et al., 1996; Merola et al., 2001), the immunochemical significance of an alternative form of the E1–E2 complex is unknown. In this regard, it is perhaps noteworthy that the human MAbs that weakly bind the E1–E2 complex in our studies have previously been described as broad in their specificity, recognizing determinants conserved between genotypes 1a and 1b (Hadlock et al., 2000). In other studies, however, gaps in this broad pattern of recognition have been observed (Cocquerel et al., 2003; Triyatni et al., 2002). The immunochemical differences noted in the literature may well be related to the genetic diversity among isolates or to the cell culture system used for recombinant expression. Based on our studies, we suggest that antigenic differences may also reflect the topologic flexibility of the HCV E1 glycoprotein. Although we cannot explain the apparent preference for the polytopic form in our studies, our findings raise the possibility that the topologic flexibility of the HCV E1 glycoprotein may play a role in immune evasion.

One might imagine that topologic flexibility in the E1–E2 complex could serve to direct the antibody response away from critical and conserved elements of the viral envelope spike. This concept has been best advanced in the case of the HIV envelope glycoprotein, where the antibody response is directed predominantly to variable epitopes displayed only on the monomeric gp120 subunit (Moore and Ho, 1995; Parren et al., 1997; Parren et al., 1999). Epitopes that give rise to rare broadly neutralizing anti-HIV MAbs appear to be physically and conformationally occluded within the oligomeric gp120–gp41 complex (Cao et al., 1997; Kwong et al., 2002; Saphire et al., 2001; Wyatt et al., 1995). By exposing antigenically variable determinants and minimizing conserved epitopes, HIV and HCV may be utilizing a common strategy, albeit via distinct mechanisms, to evade the immune response towards the establishment of chronic infection.

The task of designing an effective and much-needed HCV vaccine is complicated by the paucity of knowledge regarding the structure and function of the native HCV envelope glycoprotein complex. Recently, several laboratories have reported that infectious pseudotyped virions bearing the HCV E1–E2 complex can be generated in cell culture (Bartosch et al., 2003; Drummer et al., 2003; Hsu et al., 2003) and it is possible that this methodology may be refined to enable the biochemical and immunochemical dissection of the functional HCV envelope glycoprotein complex. In this regard, it may be important to consider the role of an alternative E1 glycoprotein topology in HCV biology and pathogenesis.

Acknowledgements

We thank Zhen-Yong Keck and Steven K. H. Foung (Stanford University) for providing human anti-E1 and anti-E2 MAbs and for valuable discussions throughout this project. Other reagents were kindly provided by S. Levy (Stanford University), J. Lau (Ribapharm), S. Zolla-Pazner (New York University), M. Posner (Harvard University) and G. Lewis (University of Maryland). This work was supported by the National Institutes of Health Grant R03 AI054388 to Jack H. Nunberg.

References

Abacioglu, Y.H., Fouts, T.R., Laman, J.D., Claassen, E., Pincus, S.H., Moore, J.P., Roby, C.A., Kamin-Lewis, R., Lewis, G.K., 1994. Epitope mapping and topology of baculovirus-expressed HIV-1 gp160 determined with a panel of murine monoclonal antibodies. AIDS Res. Hum. Retroviruses 10, 371–381.

Aizaki, H., Aoki, Y., Harada, T., Ishii, K., Suzuki, T., Nagamori, S., Toda, G., Matsuura, Y., Miyamura, T., 1998. Full-length complementary DNA of hepatitis C virus genome from an infectious blood sample. Hepatology 27, 621–627.

Babcock, G.J., Mirzabekov, T., Wojtowicz, W., Sodroski, J., 2001. Ligand-binding characteristics of CXCR4 incorporated into paramagnetic proteoliposomes. J. Biol. Chem. 276, 38,433–38,440.

Bartenschlager, R., Lohmann, V., 2001. Novel cell culture systems for the hepatitis C virus. Antiviral Res. 52, 1–17.

Bartosch, B., Dubuisson, J., Cosset, F.L., 2003. Infectious hepatitis C virus pseudo-particles containing functional E1–E2 envelope protein complexes. J. Exp. Med. 197, 633–642.

Cao, J., Sullivan, N., Desjardin, E., Parolin, C., Robinson, J., Wyatt, R., Sodroski, J., 1997. Replication and neutralization of human immunodeficiency virus type 1 lacking the V1 and V2 variable loops of the gp120 envelope glycoprotein. J. Virol. 71, 9808–9812.

Carrere-Kremer, S., Montpellier-Pala, C., Cocquerel, L., Wychowski, C., Penin, F., Dubuisson, J., 2002. Subcellular localization and topology of the p7 polypeptide of hepatitis C virus. J. Virol. 76, 3720–3730.

Cavacini, L.A., Emes, C.L., Wisnewski, A.V., Power, J., Lewis, G., Montefiori, D., Posner, M.R., 1998. Functional and molecular characterization of human monoclonal antibody reactive with the immunodominant region of HIV type 1 glycoprotein 41. AIDS Res. Hum. Retroviruses 14, 1271–1280.

Choukhi, A., Ung, S., Wychowski, C., Dubuisson, J., 1998. Involvement of endoplasmic reticulum chaperones in the folding of hepatitis C virus glycoproteins. J. Virol. 72, 3851–3858.

Cocquerel, L., Meunier, J.C., Pillez, A., Wychowski, C., Dubuisson, J., 1998. A retention signal necessary and sufficient for endoplasmic reticulum localization maps to the transmembrane domain of hepatitis C virus glycoprotein E2. J. Virol. 72, 2183–2191.

Cocquerel, L., Duvet, S., Meunier, J.C., Pillez, A., Cacan, R., Wychowski, C., Dubuisson, J., 1999. The transmembrane domain of hepatitis C virus glycoprotein E1 is a signal for static retention in the endoplasmic reticulum. J. Virol. 73, 2641–2649.

Cocquerel, L., Wychowski, C., Minner, F., Penin, F., Dubuisson, J., 2000. Charged residues in the transmembrane domains of hepatitis C virus glycoproteins play a major role in the processing, subcellular localization, and assembly of these envelope proteins. J. Virol. 74, 3623–3633.

Cocquerel, L., Op de Beeck, A., Lambot, M., Roussel, J., Delgrange, D., Pillez, A., Wychowski, C., Penin, F., Dubuisson, J., 2002. Topological changes in the transmembrane domains of hepatitis C virus envelope glycoproteins. EMBO J. 21, 2893–2902.

Cocquerel, L., Quinn, E.R., Flint, M., Hadlock, K.G., Foung, S.K., Levy, S., 2003. Recognition of native hepatitis C virus E1E2 heterodimers by a human monoclonal antibody. J. Virol. 77, 1604–1609.

Columbia University Bioinformatics Center, 2002. PredictProtein.

Conley, A.J., Gorny, M.K., Kessler II, J.A., Boots, L.J., Ossorio-Castro, M., Koenig, S., Lineberger, D.W., Emini, E.A., Williams, C., Zolla-Pazner, S., 1994. Neutralization of primary human immunodeficiency virus type 1 isolates by the broadly reactive anti-V3 monoclonal antibody, 447-52D. J. Virol. 68, 6994–7000.

Deleersnyder, V., Pillez, A., Wychowski, C., Blight, K., Xu, J., Hahn, Y.S., Rice, C.M., Dubuisson, J., 1997. Formation of native hepatitis C virus glycoprotein complexes. J. Virol. 71, 697–704.

Drummer, H.E., Maerz, A., Poumbourios, P., 2003. Cell surface expression of functional hepatitis C virus E1 and E2 glycoproteins. FEBS Lett. 546, 385–390.

Dubuisson, J., 2000. Folding, assembly and subcellular localization of hepatitis C virus glycoproteins. Curr. Top. Microbiol. Immunol. 242, 135–148.

Dubuisson, J., Hsu, H.H., Cheung, R.C., Greenberg, H.B., Russell, D.G., Rice, C.M., 1994. Formation and intracellular localization of hepatitis C virus envelope glycoprotein complexes expressed by recombinant vaccinia and Sindbis viruses. J. Virol. 68, 6147–6160.

Dubuisson, J., Rice, C.M., 1996. Hepatitis C virus glycoprotein folding: disulfide bond formation and association with calnexin. J. Virol. 70, 778–786.

Duvet, S., Cocquerel, L., Pillez, A., Cacan, R., Verbert, A., Moradpour, D., Wychowski, C., Dubuisson, J., 1998. Hepatitis C virus glycoprotein complex localization in the endoplasmic reticulum involves a determinant for retention and not retrieval. J. Biol. Chem. 273, 32,088–32,095.

Flint, M., Maidens, C., Loomis-Price, L.D., Shotton, C., Dubuisson, J., Monk, P., Higginbottom, A., Levy, S., McKeating, J.A., 1999. Characterization of hepatitis C virus E2 glycoprotein interaction with a putative cellular receptor, CD81. J. Virol. 73, 6235–6244.

Flint, M., McKeating, J.A., 1999. The C-terminal region of the hepatitis C virus E1 glycoprotein confers localization within the endoplasmic reticulum. J. Gen. Virol. 80, 1943–1947.

Gallina, A., Hanley, T.M., Mandel, R., Trahey, M., Broder, C.C., Viglianti, G.A., Ryser, H.J., 2002. Inhibitors of protein-disulfide isomerase prevent cleavage of disulfide bonds in receptor-bound glycoprotein 120 and prevent HIV-1 entry. J. Biol. Chem. 277, 50,579–50,588.

Grakoui, A., Wychowski, C., Lin, C., Feinstone, S.M., Rice, C.M., 1993. Expression and identification of hepatitis C virus polyprotein cleavage products. J. Virol. 67, 1385–1395.

Grundner, C., Mirzabekov, T., Sodroski, J., Wyatt, R., 2002. Solid-phase proteoliposomes containing human immunodeficiency virus envelope glycoproteins. J. Virol. 76, 3511–3521.

Hadlock, K.G., Lanford, R.E., Perkins, S., Rowe, J., Yang, Q., Levy, S., Pileri, P., Abrignani, S., Foung, S.K., 2000. Human monoclonal antibodies that inhibit binding of hepatitis C virus E2 protein to CD81 and recognize conserved conformational epitopes. J. Virol. 74, 10,407–10,416.

Hsu, M., Zhang, J., Flint, M., Logvinoff, C., Cheng-Mayer, C., Rice, C.M., McKeating, J.A., 2003. Hepatitis C virus glycoproteins mediate pH-dependent cell entry of pseudotyped retroviral particles. Proc. Natl. Acad. Sci. U. S. A. 100, 7271–7276.

Kim, J.-S., Raines, R.T., 1993. Ribonuclease S-peptide as a carrier in fusion proteins. Prot. Sci. 2, 348–356.

Kwong, P.D., Doyle, M.L., Casper, D.J., Cicala, C., Leavitt, S.A., Majeed, S., Steenbeke, T.D., Venturi, M., Chaiken, I., Fung, M., Katinger, H., Parren, P.W., Robinson, J., Van Ryk, D., Wang, L., Burton, D.R., Freire, E., Wyatt, R., Sodroski, J., Hendrickson, W.A., Arthos, J., 2002. HIV-1 evades antibody-mediated neutralization through conformational masking of receptor-binding sites. Nature 420, 678–682.

Lambert, C., Prange, R., 2001. Dual topology of the hepatitis B virus large envelope protein: determinants influencing post-translational pre-S translocation. J. Biol. Chem. 276, 22,265–22,272.

Lin, C., Lindenbach, B.D., Pragai, B.M., McCourt, D.W., Rice, C.M., 1994. Processing in the hepatitis C virus E2-NS2 region: identification of p7 and two distinct E2-specific products with different C termini. J. Virol. 68, 5063–5073.

Lo, S.Y., Selby, M.J., Ou, J.H., 1996. Interaction between hepatitis C virus core protein and E1 envelope protein. J. Virol. 70, 5177–5182.

Lu, M., Stoller, M.O., Wang, S., Liu, J., Fagan, M.B., Nunberg, J.H., 2001. Structural and functional analysis of interhelical interactions in the HIV-1 gp41 envelope glycoprotein by alanine-scanning mutagenesis. J. Virol. 75, 11,146–11,156.

Matsuura, Y., Suzuki, T., Suzuki, R., Sato, M., Aizaki, H., Saito, I., Miyamura, T., 1994. Processing of E1 and E2 glycoproteins of hepatitis C virus expressed in mammalian and insect cells. Virology 205, 141–150.

McGinnes, L.W., Reitter, J.N., Gravel, K., Morrison, T.G., 2003. Evidence for mixed membrane topology of the Newcastle disease virus fusion protein. J. Virol. 77, 1951–1963.

Merola, M., Brazzoli, M., Cocchiarella, F., Heile, J.M., Helenius, A., Weiner, A.J., Houghton, M., Abrignani, S., 2001. Folding of hepatitis C virus E1 glycoprotein in a cell-free system. J. Virol. 75, 11,205–11,217.

Meunier, J.C., Fournillier, A., Choukhi, A., Cahour, A., Cocquerel, L., Dubuisson, J., Wychowski, C., 1999. Analysis of the glycosylation sites of Hepatitis C virus (HCV) glycoprotein E1 and the influence of E1 glycans on the formation of the HCV glycoprotein complex. J. Gen. Virol. 80, 887–896.

Michalak, J.P., Wychowski, C., Choukhi, A., Meunier, J.C., Ung, S., Rice, C.M., Dubuisson, J., 1997. Characterization of truncated forms of hepatitis C virus glycoproteins. J. Gen. Virol. 78, 2299–2306.

Mirzabekov, T., Kontos, H., Farzan, M., Marasco, W., Sodroski, J., 2000. Paramagnetic proteoliposomes containing a pure, native, and oriented seven-transmembrane segment protein, CCR5. Nat. Biotech. 18, 649–654.

Mizushima, H., Hijikata, M., Asabe, S., Hirota, M., Kimura, K., Shimotohno, K., 1994. Two hepatitis C virus glycoprotein E2 products with different C termini. J. Virol. 68, 6215–6222.

Moore, J.P., Ho, D.D., 1995. HIV-1 neutralization: the consequences of viral adaptation to growth on transformed T cells. AIDS 9 (Suppl. A), S117–S136.

Op De Beeck, A., Montserret, R., Duvet, S., Cocquerel, L., Cacan, R., Barberot, B., Le Maire, M., Penin, F., Dubuisson, J., 2000. The transmembrane domains of hepatitis C virus envelope glycoproteins E1 and E2 play a major role in heterodimerization. J. Biol. Chem. 275, 31,428–31,437.

Op De Beeck, A., Cocquerel, L., Dubuisson, J., 2001. Biogenesis of hepatitis C virus envelope glycoproteins. J. Gen. Virol. 82, 2589–2595.

Parren, P.W., Gauduin, M.C., Koup, R.A., Poignard, P., Sattentau, Q.J., Fisicaro, P., Burton, D.R., 1997. Relevance of the antibody response against human immunodeficiency virus type 1 envelope to vaccine design. Immunol. Lett. 58, 125–132.

Parren, P.W.H.I., Moore, J.P., Burton, D.R., Sattentau, Q.J., 1999. The neutralizing antibody response to HIV-1: viral evasion and escape from humoral immunity. AIDS 13 (Suppl. A), S137–S162.

Patel, J., Patel, A.H., McLauchlan, J., 2001. The transmembrane domain of the hepatitis C virus E2 glycoprotein is required for correct folding of the E1 glycoprotein and native complex formation. Virology 279, 58–68.

Reed, K.E., Rice, C.M., 2000. Overview of hepatitis C virus genome structure, polyprotein processing, and protein properties. Curr. Top. Microbiol. Immunol. 242, 55–84.

Richards, F.M., Vithayathil, P.J., 1959. The preparation of subtilisin-modified ribonuclease and the separation of the peptide and protein components. J. Biol. Chem. 234, 1459–1465.

Rigaud, J.L., Pitard, B., Levy, D., 1995. Reconstitution of membrane proteins into liposomes: application to energy-transducing membrane proteins. Biochem. Biophys. Acta 1231, 223–246.

Roccasecca, R., Ansuini, H., Vitelli, A., Meola, A., Scarselli, E., Acali, S., Pezzanera, M., Ercole, B.B., McKeating, J., Yagnik, A., Lahm, A., Tramontano, A., Cortese, R., Nicosia, A., 2003. Binding of the hepatitis C virus E2 glycoprotein to CD81 is strain specific and is modulated by a complex interplay between hypervariable regions 1 and 2. J. Virol. 77, 1856–1867.

Rost, B., Casadio, R., Fariselli, P., Sander, C., 1995. Transmembrane helices predicted at 95% accuracy. Prot. Sci. 4, 521–533.

Saphire, E.O., Parren, P.W., Pantophlet, R., Zwick, M.B., Morris, G.M., Rudd, P.M., Dwek, R.A., Stanfield, R.L., Burton, D.R., Wilson, I.A., 2001. Crystal structure of a neutralizing human IGG against HIV-1: a template for vaccine design. Science 293, 1155–1159.

Selby, M.J., Choo, Q.L., Berger, K., Kuo, G., Glazer, E., Eckart, M., Lee, C., Chien, D., Kuo, C., Houghton, M., 1993. Expression, identification and subcellular localization of the proteins encoded by the hepatitis C viral genome. J. Gen. Virol. 74, 1103–1113.

Takikawa, S., Ishii, K., Aizaki, H., Suzuki, T., Asakura, H., Matsuura, Y., Miyamura, T., 2000. Cell fusion activity of hepatitis C virus envelope proteins. J. Virol. 74, 5066–5074.

Tatu, U., Braakman, I., Helenius, A., 1993. Membrane glycoprotein folding, oligomerization and intracellular transport: effects of dithiothreitol in living cells. EMBO J. 12, 2151–2157.

Triyatni, M., Vergalla, J., Davis, A.R., Hadlock, K.G., Foung, S.K., Liang, T.J., 2002. Structural features of envelope proteins on hepatitis C virus-like particles as determined by anti-envelope monoclonal antibodies and CD81 binding. Virology 298, 124–132.

von Heijne, G., 1988. Transcending the impenetrable: how proteins come to terms with membranes. Biochim. Biophys. Acta 947, 307–333.

Walter, A., Eidelman, O., Ollivon, M., Blumenthal, R., 1990. Functional reconstitution of viral envelopes. In: "Membrane Fusion" Wilschut, J., Hoekstra, D. (Eds.), Marcel Dekker, Inc., pp. 395–418.

World Health Organization, 1999. Global surveillance and control of hepatitis C. J. Viral Hepatitis 6, 35–47.

Wyatt, R., Moore, J.P., Accola, M., Desjardin, E., Robinson, J., Sodroski, J., 1995. Involvement of the V1/V2 variable loop structure in the exposure of human immunodeficiency virus type 1 gp120 epitopes induced by receptor binding. J. Virol. 69, 5723–5733.

Yagnik, A.T., Lahm, A., Meola, A., Roccasecca, R.M., Ercole, B.B., Nicosia, A., Tramontano, A., 2000. A model for the hepatitis C virus envelope glycoprotein E2. Proteins 40, 355–366.

JOURNAL OF VIROLOGY, Jan. 2005, p. 1271–1281 Vol. 79, No. 2
0022-538X/05/$08.00+0 doi:10.1128/JVI.79.2.1271–1281.2005

Molecular Determinants for Subcellular Localization of Hepatitis C Virus Core Protein

Ryosuke Suzuki,[1] Shinichiro Sakamoto,[1] Takeya Tsutsumi,[1] Akiko Rikimaru,[1,2] Keiko Tanaka,[3] Takashi Shimoike,[1] Kohji Moriishi,[4] Takuya Iwasaki,[3,5] Kiyohisa Mizumoto,[2] Yoshiharu Matsuura,[4] Tatsuo Miyamura,[1] and Tetsuro Suzuki[1]*

Department of Virology II, National Institute of Infectious Diseases, Shinjuku-ku,[1] Department of Biochemistry, School of Pharmaceutical Sciences, Kitasato University, Minato-ku,[2] and Department of Pathology, National Institute of Infectious Diseases, Shinjuku-ku,[3] Tokyo, Research Center for Emerging Infectious Diseases, Research Institute for Microbial Diseases, Osaka University, Suita-shi, Osaka,[4] and Department of Pathology, Institute of Tropical Medicine, Nagasaki University, Nagasaki-shi, Nagasaki,[5] Japan

Received 21 June 2004/Accepted 26 July 2004

Hepatitis C virus (HCV) core protein is a putative nucleocapsid protein with a number of regulatory functions. In tissue culture cells, HCV core protein is mainly located at the endoplasmic reticulum as well as mitochondria and lipid droplets within the cytoplasm. However, it is also detected in the nucleus in some cells. To elucidate the mechanisms by which cellular trafficking of the protein is controlled, we performed subcellular fractionation experiments and used confocal microscopy to examine the distribution of heterologously expressed fusion proteins involving various deletions and point mutations of the HCV core combined with green fluorescent proteins. We demonstrated that a region spanning amino acids 112 to 152 can mediate association of the core protein not only with the ER but also with the mitochondrial outer membrane. This region contains an 18-amino-acid motif which is predicted to form an amphipathic α-helix structure. With regard to the nuclear targeting of the core protein, we identified a novel bipartite nuclear localization signal, which requires two out of three basic-residue clusters for efficient nuclear translocation, possibly by occupying binding sites on importin-α. Differences in the cellular trafficking of HCV core protein, achieved and maintained by multiple targeting functions as mentioned above, may in part regulate the diverse range of biological roles of the core protein.

Hepatitis C virus (HCV), the most important causative agent of posttransfusion and sporadic non-A, non-B hepatitis, is a positive-stranded RNA virus belonging to the family *Flaviviridae* (7). A precursor polyprotein of about 3,000 amino acids is encoded by a large open reading frame of the genome and undergoes cellular and viral protease-mediated posttranslational modification to produce a series of structural and nonstructural proteins (8, 13, 16).

HCV core protein, which is derived from the N terminus of the viral polyprotein, forms multimers and interacts physically with the viral RNA to constitute the nucleocapsid (28, 47, 50). Tissue transglutaminase is responsible for stabilizing the core protein by cross-linking it into a dimeric form (26). In addition, the core viral protein has properties which enable it to modulate a number of cellular processes, including transcription, inhibition or stimulation of apoptosis, and suppression of host immunity, as reviewed previously (21, 29, 51, 52). Several studies suggest that expression of the core protein affects mitochondrial function and lipid metabolism. The core protein increases the cellular production of reactive oxygen species with subsequent increases in lipid peroxidation (35, 39). The viral protein also colocalizes with human apolipoprotein AII, associates with lipid droplets, and has the capacity to influence metabolic events involving lipid storage (2, 17, 30, 36, 44). In addition, the core protein reduces microsomal triglyceride transfer, leading to defects in very low density lipoprotein assembly and secretion (40). Furthermore, the HCV core protein has transforming potential in some cells under certain conditions (5, 42). Transgenic mice expressing this protein in the liver develop hepatic steatosis due to increased oxidative stress in the absence of inflammation, with subsequent development of hepatocellular carcinoma (34, 36). These results suggest that the HCV core protein might play a pivotal role in the pathogenesis of hepatitis C in addition to its role as a structural component of the viral capsid.

The amino acid sequence of the core protein is well conserved among different HCV isolates and genotypes compared to other HCV proteins. The N-terminal domain of the HCV core protein is highly basic, while its C terminus is hydrophobic. Although several core proteins of various sizes exist (17 to 23 kDa) (15, 23, 25, 49, 56), two processing events result in the predominant production of a 21-kDa core protein. Both of these events utilize the endoplasmic reticulum (ER). The first one is to be cleaved from downstream envelope protein E1 at position 191, where the C-terminal hydrophobic domain serves as a putative signal peptide sequence. Subsequently, the signal sequence of 13 or 18 residues is processed by signal peptide peptidase (19, 23, 56).

The HCV core protein is found primarily within the membranes of cytoplasmic organelles, but it is also found in the nucleus (23, 48, 56). Immunofluorescence studies show a punc-

* Corresponding author. Mailing address: Department of Virology II, National Institute of Infectious Diseases, 1-23-1 Toyama, Shinjuku-ku, Tokyo, Japan 162-8640. Phone: (81) 3-5285-1111. Fax: (81) 3-5285-1161. E-mail: tesuzuki@nih.go.jp.

tate pattern, consistent with ER localization, as well as perinuclear localization (15, 24, 32, 46, 56). Some studies suggest direct effects of the core protein on mitochondrial function. In fact, the core protein localizes to the mitochondria (34, 39). The N-terminal domain of the core protein contains three stretches of arginine- and lysine-rich sequences. Translocation of the core protein to the nucleus, mediated by these basic-residue stretches which function as nuclear localization signals (NLSs), is observed (6, 48). In addition, Moriishi et al. demonstrated that the N-terminal region of the core protein is also essential for nuclear retention through its interaction with the proteasome activator PA28γ (33).

In this study, we found a region that is important for localization of the mature core protein to the ER and to the mitochondrial outer membrane. We also identified a novel bipartite NLS responsible for nuclear targeting of the core protein, presumably via an importin-dependent pathway.

MATERIALS AND METHODS

Plasmid construction. The construction of a plasmid expressing the full-length core protein of 191 amino acids, pCAGC191, was described previously (49). pGFP, a construct expressing green fluorescent protein (GFP) with a C-terminal Myc epitope tag sequences, was prepared as follows. pCMV/Myc/mito/GFP (Invitrogen Corp., Carlsbad, Calif.) was digested with PmlI, followed by treatment with the Klenow fragment of DNA polymerase I. The resultant linear fragment was ligated to a PstI linker (GCTGCAGC) and digested with PstI to remove the mitochondrial targeting signal sequence, followed by self-ligation. A series of HCV core-GFP fusion constructs were made by amplifying the core gene fragments with PCR with primers containing Flag epitope tag sequences (sense) and a PstI site (both). After digestion with PstI, the segments were inserted into the PstI site of pGFP. A series of GFP-core-E1 fusion constructs were made by amplifying core and E1 gene fragments with PCR with primers containing a NotI site. After digestion with NotI, the segments were inserted into the NotI site of pGFP.

pGEX-4T-1 (Amersham Bioscience Corp., Piscataway, N.J.) was used to express core protein fused with glutathione *S*-transferase (GST) in *Escherichia coli*. Core cDNA fragments encoding amino acids 1 to 71 were inserted into the EcoRI site of pGEX-4T-1. Alanine substitutions were introduced into the core protein by PCR mutagenesis with primers containing base alterations. The PCR products were then cloned into pCR2.1 (Invitrogen Corp.) and verified by DNA sequencing. Individual cDNAs were excised and inserted separately into pGFP or pGEX-4T-1. The primer sequences used in this study are available from the authors upon request.

Plasmid pRSET-hSRP1α (54), containing importin-α cDNA under the control of a T7 promoter, was kindly provided by Karsten Weis (University of California, Berkeley). A cDNA clone of importin-α possessing 14 residues (MYPYDVP DYGGGGS), derived in part from the hemagglutinin (HA) tag at the N terminus, was constructed by PCR. The resultant linear fragment was inserted under the control of a CAG promoter of pCAGGS and designated pCAG-HA-imp.

Cell culture and transfection. Human embryonic kidney 293T cells were maintained in Dulbecco's modified Eagle's medium supplemented with 100 units of penicillin per ml, 100 μg of streptomycin per ml, and 10% fetal bovine serum at 37°C in a 5% CO_2 incubator. Monolayers of 293T cells were transfected with plasmid DNA in the presence of Lipofectamine (Gibco-BRL, Life Technologies, Gaithersburg, Md.) according to the manufacturer's instructions.

Confocal immunofluorescence microscopy. Transfected cells were grown on glass coverslips. Two days after transfection, cells were fixed with 4% paraformaldehyde in phosphate-buffered saline (PBS) for 20 min at room temperature. Intracellular localization of HCV core-GFP fusion proteins was visualized in cells transfected with a variety of GFP fusion constructs.

In order to detect the HCV core protein by immunofluorescence, fixed cells were permeabilized with 0.2% Triton X-100 in PBS for 3 min at room temperature, followed by blocking with a nonfat milk solution (Block Ace; Snow Brand Milk Products Co., Sapporo, Japan). The cells were then incubated with anticore monoclonal antibody B2 (Anogen, Mississauga, Canada) for 60 min at room temperature, followed by incubation with fluorescein isothiocyanate-conjugated rabbit anti-mouse immunoglobulin G (IgG) (ICN Pharmaceuticals, Aurora, Ohio) for 45 min. To visualize mitochondria, MitoTracker Red CM-H_2XRos (Molecular Probes, Eugene, Oreg.) was added to the culture medium to a final concentration of 100 nM and incubated for 120 min at 37°C prior to fixation. To visualize the ER, goat anticalregulin antibody (Santa Cruz Biotechnology, Santa Cruz, Calif.) and rhodamine-conjugated rabbit anti-goat IgG (ICN Pharmaceuticals) were used as the first and second antibodies, respectively. To visualize HA-importin-α, mouse anti-HA antibody (Roche Molecular Biochemicals, Indianapolis, Ind.) and rhodamine-conjugated goat anti-mouse IgG (ICN Pharmaceuticals) were used as the first and second antibodies, respectively. All specimens were examined with an LSM510 laser scanning confocal microscope (Carl Zeiss, Oberkochen, Germany).

Immunoelectron microscopy. Cells were transfected as described above. After 2 days, cells were fixed with 3% paraformaldehyde and 0.1% glutaraldehyde in 0.1 M PBS (pH 7.4). Free aldehyde groups were quenched with 50 mM NH_4Cl in PBS. The cell pellets were embedded at progressively lower temperatures (down to −35°C) in Lowicryl k4M according to an established protocol (43). Ultrathin sections were prepared and mounted on carbon-coated nickel grids. To perform electron microscopy, Lowicryl k4M ultrathin sections, mounted on grids, were floated on a droplet of PBS containing 1% bovine serum albumin, 0.1% Triton X-100, and 0.1% Tween 20 for 10 min, after which they were exposed to droplets of mouse anticore monoclonal antibody (Anogen) diluted in PBS for 45 min. Following this, they were rinsed twice for 5 min each in PBS and incubated with anti-mouse IgG-coated 10-nm immunogold particles (British Biocell, Cardiff, United Kingdom) for 45 min. After rinsing with PBS and distilled water, the grids and embedded sections were air dried and exposed to uranyl and lead acetate contrast agents.

Subcellular fractionation. All steps were performed at 4°C in the presence of a protease inhibitor cocktail called Complete (Roche Molecular Biochemicals). To isolate the ER fraction, transfected cells were washed with PBS, lysed in homogenization buffer A (50 mM Tris-HCl [pH 8.0], 1 mM β-mercaptoethanol, 1 mM EDTA, and 0.32 M sucrose), and then centrifuged at 5,000 × *g* for 10 min. The supernatant was then collected and centrifuged at 105,000 × *g* for 1 h. The pellet was disrupted in lysis buffer (50 mM Tris-HCl [pH 7.5], 150 mM NaCl, 1% NP-40, 1 mM dithiothreitol, 1 mM sodium orthovanadate, and 10 mM sodium fluoride), after which it was centrifuged at 15,000 × *g* for 20 min. The resulting supernatant was used as the ER fraction.

To isolate the mitochondrial fraction, transfected cells were washed with PBS and homogenized in ice-cold homogenization buffer B (200 mM mannitol, 50 mM sucrose, 1 mM EDTA, and 10 mM Tris-HCl) at pH 7.4. The supernatant was then centrifuged at 1,000 × *g* for 10 min to remove large debris and nuclei. The resulting supernatant was then centrifuged at 20,000 × *g* for 20 min to obtain crude mitochondria. The crude mitochondria pellet was subfractionated in Nycodenz gradients for further purification of mitochondria. Nycodenz (Axis-Shield PoC AS, Oslo, Norway) solution at 50% (wt/vol) was prepared in buffer containing 5 mM Tris-HCl and 1 mM EDTA at pH 7.4. This stock solution was then diluted with buffer containing 0.25 M sucrose, 5 mM Tris-HCl, and 1 mM EDTA at pH 7.4 before use. The crude mitochondrial pellets was suspended in 4 ml of 25% Nycodenz solution and overlaid onto the following discontinuous Nycodenz gradients: 1 ml of 40%, 1 ml of 34%, and 2 ml of 30%. The samples were topped off with 2 ml of 23% Nycodenz solution after placement onto the discontinuous gradients. The tubes were then centrifuged at 52,000 × *g* for 90 min. The dense band seen after centrifugation at the 25 to 30% interface was recovered as the purified mitochondrial fraction.

To determine the submitochondrial localization pattern of the core protein, mitochondria were resuspended in SH buffer (0.6 M sorbitol and 20 mM HEPES-KOH [pH 7.2]) in the absence or presence of 30 μg of proteinase K per ml after purification by Nycodenz density gradient centrifugation. Samples were incubated for 30 min at 0°C, after which protease digestion was halted by the addition of *p*-aminophenyl methanesulfonyl fluoride hydrochloride (*p*-APMSF) (5 mM). Proteins lysed in sodium dodecyl sulfate (SDS) sample buffer were analyzed by SDS-polyacrylamide gel electrophoresis (PAGE) and immunoblotted as described below.

Immunoblot analysis. The proteins were transferred to a polyvinylidene difluoride membrane (Immobilon; Millipore, Tokyo, Japan) after separation by SDS-PAGE. After blocking, the membranes were probed with monoclonal- or polyclonal-antibody against core protein (Anogen), prohibitin (Neo Markers, Fremont, Calif.), ribophorin I (Santa Cruz Biotechnology), translocase of the outer membrane (Tom) 20 (Santa Cruz Biotechnology), translocase of the inner membrane (Tim) 17 (Santa Cruz Biotechnology), or GFP (Santa Cruz Biotechnology). Immunoblots were developed as previously described (15).

GST pulldown assay. *Escherichia coli* BL21 cells were transformed with GST-core fusion plasmids and grown at 37°C. Expression of the fusion protein was induced by 1 mM isopropyl-β-D-thiogalactopyranoside at 37°C for 3 h. Bacteria were harvested, suspended in lysis buffer (1% Triton X-100 in PBS), and soni-

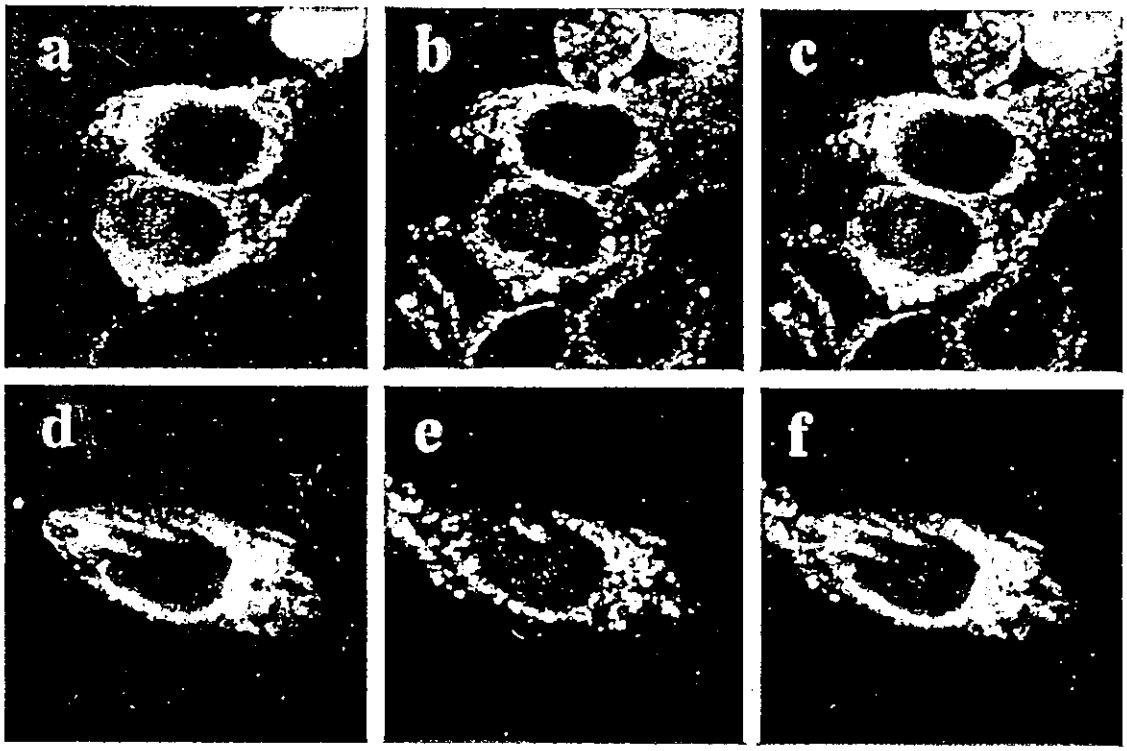

FIG. 1. Confocal analysis of double staining for HCV core protein and ER or mitochondria. 293T cells transfected with full-length HCV core expression plasmid, pCAGC191 were allowed to express the plasmid for 2 days. Transfected cells were fixed directly (a to c) or fixed after loading with Mitotracker (d to f). After permeabilization with Triton X-100, cells were subjected to immunofluorescence staining with a mouse anticore antibody. A goat anticalregulin antibody was used for ER staining. The green signals corresponding to the core were found with a fluorescein isothiocyanate-conjugated rabbit anti-mouse IgG (a and d). The red signals corresponding to the ER were obtained with a rhodamine-conjugated rabbit anti-goat IgG secondary antibody (b). Mitochondria were stained with the mitochondrion-selective dye Mitotracker (e). Overlay resulted in yellow signals indicative of colocalization (c and f).

cated on ice. GST and GST fusion proteins were purified from bacterial lysates with glutathione-Sepharose beads (Amersham Bioscience Corp.). The beads were washed four times with lysis buffer. Approximately equal amounts of purified protein, as estimated by Coomassie brilliant blue staining, were used for the binding assays. For pulldown assays, in vitro transcription and translation of importin-α was done with pRSET-hSRP1α and the TNT-coupled reticulocyte lysate system (Promega Corp., Madison, Wis.) with T7 RNA polymerase. The reaction was carried out at 30°C for 4 h in the presence of [^{35}S]methionine/cysteine (ICN Pharmaceuticals). The translation product was then incubated with glutathione-Sepharose beads bound to GST fusion proteins in 1 ml of binding buffer (40 mM HEPES [pH 7.5], 100 mM KCl, 0.1% NP-40, and 20 mM 2-mercaptoethanol) at 4°C for 1 h. The beads were washed four times with binding buffer, and the pulldown complexes were separated by SDS-PAGE on 15% polyacrylamide gels. The gels were then fixed, dried, and analyzed with autoradiography.

RESULTS

Subcellular localization of HCV core protein. To assess the subcellular localization of HCV core protein, we first analyzed cells transfected with a full-length core-expressing construct by confocal microscopy. In accordance with previous observations (2, 15, 32, 45, 56), a granular cytoplasmic staining pattern of the core protein was observed in 293T (Fig. 1) and human hepatoblastoma HepG2 (data not shown) cells. Dual staining of transfected cells with antibody against the ER protein calregulin along with anticore antibody confirmed the ER localization of the core protein (Fig. 1a, b, and c show the core,

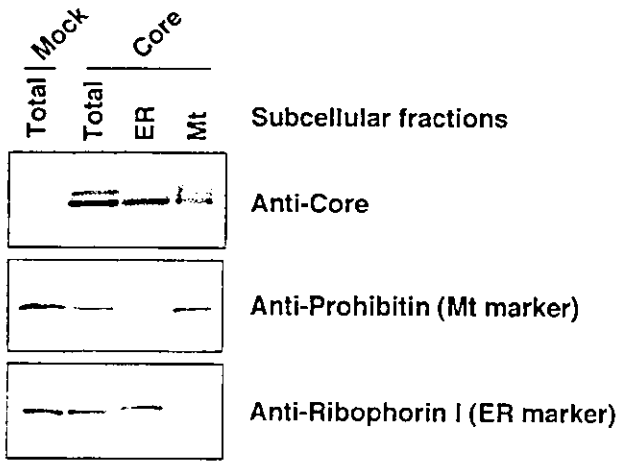

FIG. 2. Subcellular distribution of HCV core protein analyzed by immunoblotting. ER and mitochondrial (Mt) fractions were isolated from 293T cells expressing the full-length core protein (Core) or nontransfected cells (Mock) 2 days after transfection. Equal amounts of protein from each fraction as well as whole cell lysates (Total) were subjected to immunoblotting with a monoclonal antibody against either HCV core, prohibitin, or ribophorin I.

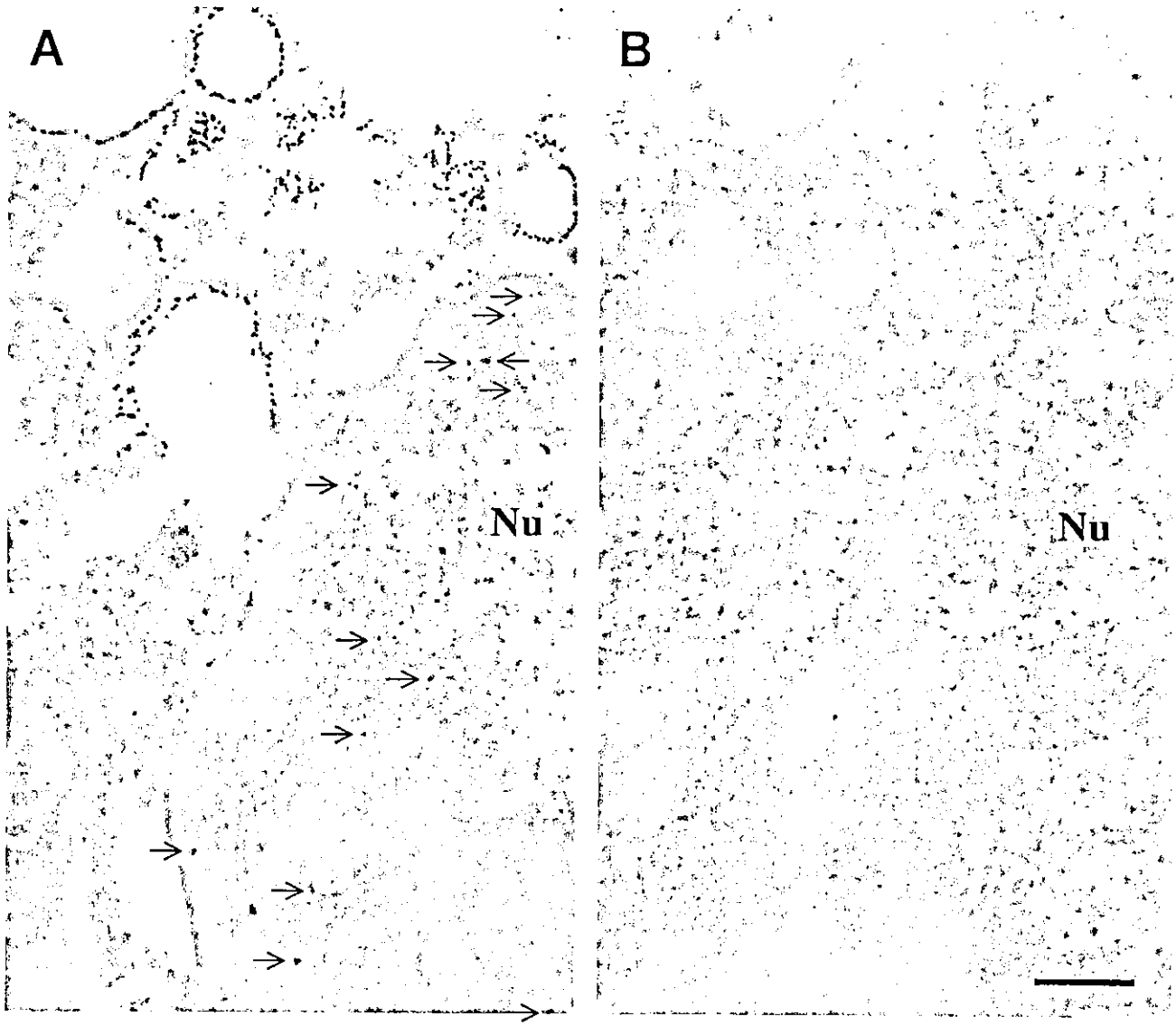

FIG. 3. Immunoelectron microscopy of HCV core protein. 293T cells expressing the full-length core protein (A) and nonexpressing cells (B) fixed 2 days after transfection. Immunoelectron microscopic analysis was performed with a mouse anticore antibody and a secondary anti-mouse IgG conjugated with gold particles. The arrows indicate the core protein localized in the nucleus (Nu). Bar, 500 nm.

calregulin, and a merged image, respectively). The pattern of subcellular localization of the core protein (Fig. 1d) was compared to the distribution of mitochondria, as revealed by MitoTracker staining (Fig. 1e). Although distribution of the core protein was not completely identical with that of the mitochondrion-selective dye, overlapping staining was observed, particularly in the perinuclear region (Fig. 1f).

Intracellular localization of the core protein was further examined in 293T cells by subcellular fractionation and Western blotting. The core protein was present in both the ER and mitochondrial fractions (Fig. 2), while it was not detected in the cytosol fraction (data not shown). The purity of the ER and mitochondrial fractions was confirmed with antibodies against ribophorin I as an ER marker and prohibitin as a mitochondrial marker.

It is generally difficult to identify the nuclear distribution of proteins of interest due to contamination of the nuclear preparation with unbroken, intact cells. Thus, to investigate whether the core protein localizes to the nucleus, we examined transfected cells by immunoelectron microscopy. Although gold particles were primarily observed within cytoplasmic membranes, perhaps highlighting the ER, immunoreactivity to anticore antibody was also observed in the nucleus (Fig. 3A, arrows). In contrast, no antibody labeling was observed in cells transfected with an empty vector (Fig. 3B).

Thus, HCV core protein predominates in the cytoplasm in a membrane-associated form(s) with ER and mitochondria, but nuclear localization is also observed.

Regions responsible for directing core protein to the ER and mitochondria. Given the tendency of the core protein to lo-

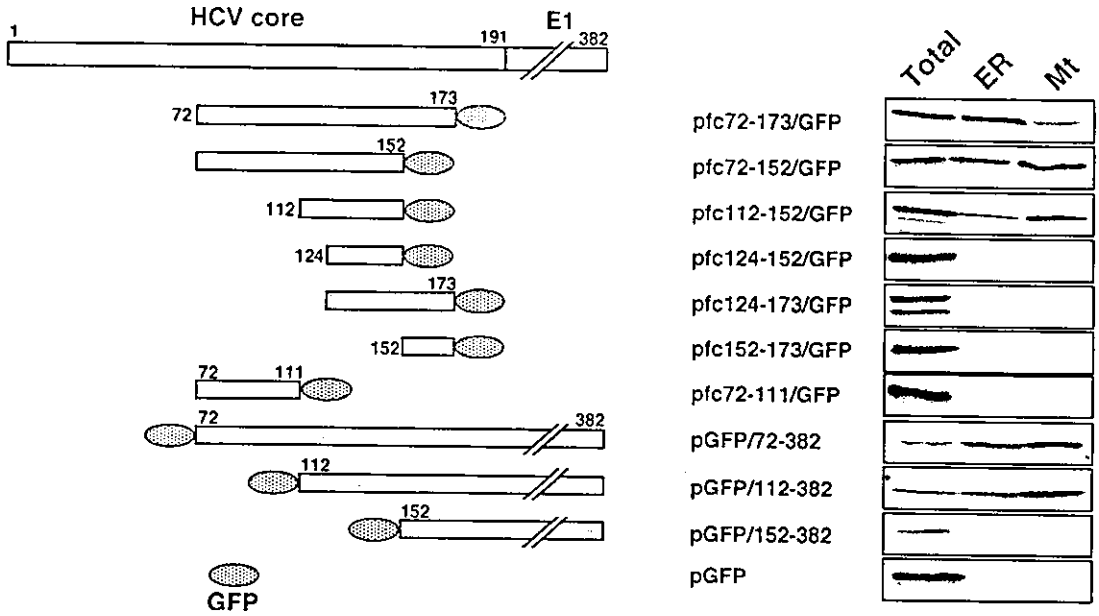

FIG. 4. Identification of segments that mediate association with ER and mitochondria in the core protein. Schematic diagram (left) and nomenclature (middle) of the core-GFP fusions are shown. Gray bars, expressed core and E1 regions. Subcellular distribution of fusion proteins is indicated on the right. ER and mitochondrial (Mt) fractions as well as whole-cell lysates (Total) were subjected to immunoblotting with an anti-GFP antibody.

calize to the ER and to mitochondria, we next investigated whether specific sequences might be responsible for transporting the core protein to these organelles. Fusion proteins between different regions of the core protein and GFP were developed, with specific emphasis on the region downstream of amino acid 72 because this region contains clusters of hydrophobic amino acids and the N-terminal 71 residues of the core are known to play a role in nuclear targeting (6, 48).

Western blotting of subcellular fractions with anti-GFP antibody revealed the localization of a core (72–173)-GFP fusion protein to the ER and to mitochondria (Fig. 4). Fusion proteins containing GFP and core proteins with N- or C-terminal deletions (72-152-GFP and 112-152-GFP) were likewise identified within the ER and mitochondrial fractions. In contrast, the ER and mitochondrial fractions did not contain GFP fusion proteins containing core protein amino acids 124 to 152, 124 to 173, 152 to 173, or 72 to 111. These fusion proteins demonstrated distribution profiles similar to that of GFP alone. We also tested GFP-core-E1 fusions, which are processed at the C terminus of the core by signal peptidase and signal peptide peptidase (19, 30). GFP-core fusions expressed from pGFP/72–382 and pGFP/112–382 were detected in the ER and mitochondrial fractions. The fusion expressed from pGFP/152–382 was not identified in these fractions.

We further analyzed subcellular localization of the fusion proteins by confocal immunofluorescence microscopy (Fig. 5). As expected, fusions of (72–173)-GFP and (112–152)-GFP exhibited localization to the ER and mitochondria. The patterns of subcellular localization of these fusions are indistinguishable from that of the full-length core protein, as shown in Fig. 1. Expression of (124–152)-GFP or (112–123)-GFP resulted in widespread diffusion of the fusion in the cell. Thus, these results indicate that the region spanning amino acids 112 to 152 can mediate association of the core protein not only to the ER but also to the mitochondria.

We subsequently examined the submitochondrial localization of the core protein with a protease protection assay. As shown in Fig. 6A, HCV core protein localized in the mitochondria was completely digested upon treatment with proteinase K for 30 min at 0°C. Under identical conditions, a marker specific for the mitochondrial outer membrane, Tom20, was also observed to disappear, whereas digestion of a mitochondrial inner membrane marker, Tim17, was not observed. These findings confirm that HCV core protein is localized to the mitochondrial outer membrane.

The predicted secondary structure of the region, amino acids 72 to 173, is shown in Fig. 6B. The presence of a long helical segment, lying between amino acids 116 and 134, and two short α-helices (amino acids 146 to 152 and amino acids 155 to 159) were predicted. The results of the cell fractionation assay and confocal microscopy with a series of deletion mutants shown in Fig. 4 and 5 suggest that an α-helix between amino acids 116 and 134 may be required for associating the core protein with the ER and the mitochondrial outer membrane. When amino acids 117 to 134 are portrayed as a helical wheel, we found an amphipathic structure with hydrophobic residues on one side and polar residues on the other side of the α-helix (Fig. 6C), which is often observed in membrane-associated proteins. This helical conformation might be important for directing the core protein to the ER and mitochondrial outer membranes.

Nuclear localization of the HCV core protein is mediated by a bipartite NLS, possibly via an importin-dependent pathway. Although HCV core protein is mainly localized within the cytoplasm, it is also found in the nucleus, as shown in Fig. 3.

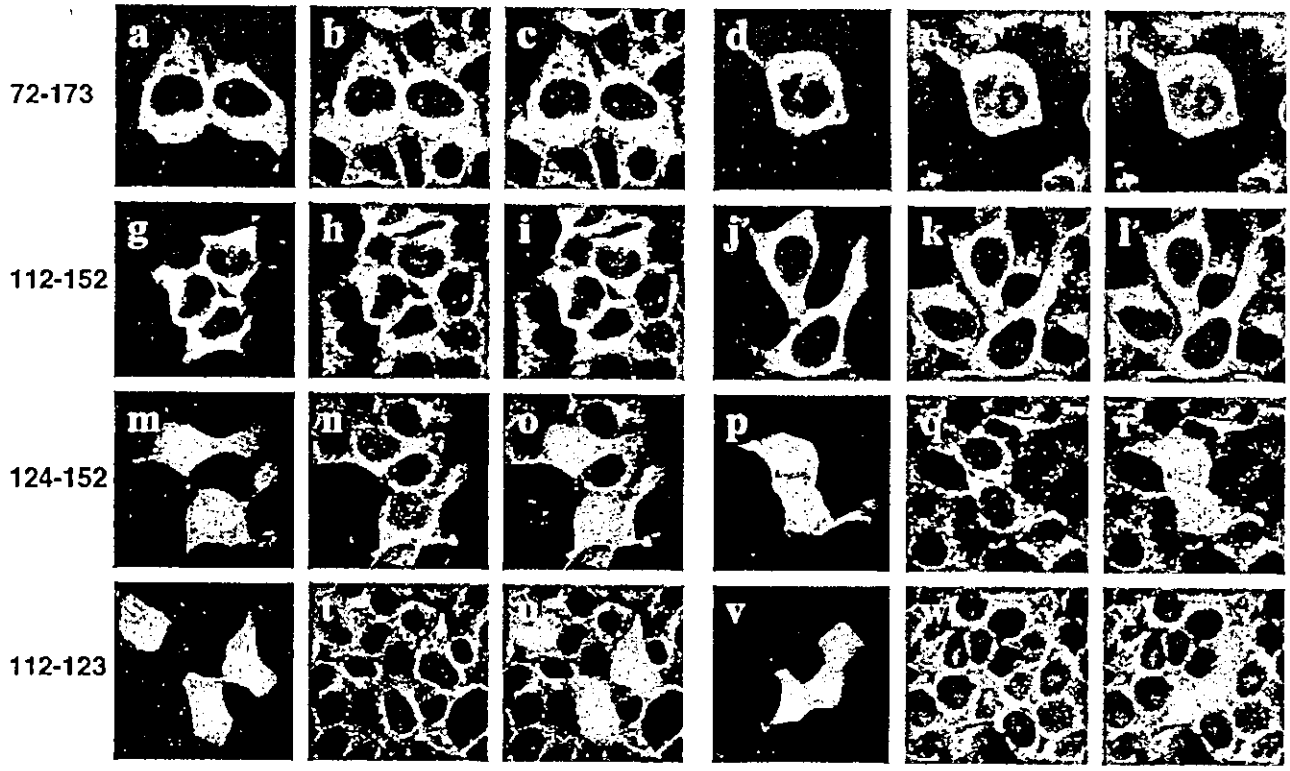

FIG. 5. Confocal analysis of double staining for core-GFP fusion protein and ER or mitochondria. 293T cells transfected with core-GFP expression plasmids (72–173, 112–152, 124–152, and 112–123) were allowed to express the plasmid for 2 days. Transfected cells were fixed directly (a to c, g to i, m to o, and s to u) or fixed after loading with Mitotracker (d to f, j to l, p to r, and v to x). After permeabilization with Triton X-100, a goat anticalregulin antibody was used for ER staining. The red signals corresponding to the ER were obtained with a rhodamine-conjugated rabbit anti-goat IgG secondary antibody (b, h, n, and t). Mitochondria were stained with the mitochondrion-selective dye Mitotracker (e, k, q, and w). Overlay resulted in yellow signals indicative of colocalization (c, f, i, l, o, r, u, and x).

The results of previous studies demonstrate that the N-terminal region of the core protein is responsible for nuclear targeting. It contains three clusters of basic amino acid residues that represent putative consensus motifs for NLS sequences PKPQRKTKR (amino acids 5 to 13), PRRGPR (amino acids 38 to 43), and PRGRRQPIPKARRP (amino acids 58 to 71) (6, 48). Nuclear targeting is generally governed by a family of transporters or cytosolic receptor proteins, known as importins or karyopherins, which function in concert with a guanine nucleotide-binding protein named Ran and other regulatory proteins such as NTF2/p10. Conventional NLS-dependent nuclear targeting occurs when importin-α recognizes the NLS sequence, mediating binding to importin-β1, after which the trimeric complex translocates to the nucleus (12).

In order to determine whether the putative NLS motifs identified within the core protein sequence are capable of binding to importin-α, we examined the in vitro interaction between bacterially expressed GST-fused core protein and ^{35}S-labeled importin-α with a GST pulldown assay. We then substituted lysine and arginine residues of one or more of the putative NLS motifs of the core protein (all contained within the first 71 amino acids of the N terminus) with alanine and fused the resultant constructs with GST, as shown schematically in Fig. 7A. As shown in Fig. 7B (upper panel), importin-α was pulled down by a GST fusion protein containing wild-type core (amino acids 1 to 71) protein but not with GST alone, suggesting that direct binding occurs between the core protein and importin-α. Importin-α was also pulled down by GST-core fusion proteins containing substitutions in one or two NLS motifs (NLS/m1, NLS/m2, NLS/m3, NLS/m4, NLS/m5, and NLS/m6). However, importin-α was not pulled down by GST-core fusion proteins containing alanine substitutions in all three NLS motifs (NLS/m7). It should be noted that similar amounts of GST fusion proteins were used for each of the in vitro pulldown assays, followed by SDS-PAGE and Coomassie brilliant blue staining (Fig. 7B, lower panel). These results demonstrated that all three putative NLS motifs of the N-terminal region of the core protein can mediate binding to importin-α, which suggests that nuclear translocation of the core protein occurs via an importin-dependent pathway (12).

The interaction between the core and importin-α was further analyzed by a colocalization assay (Fig. 7C). The GFP fusion containing the wild-type core (amino acids 1 to 71) was well colocalized with HA-importin-α; distribution of the two proteins showed similar nuclear staining patterns, confirming the presence of a functional NLS sequence(s) within the core protein. In contrast, NLS/m4, with substitutions in two NLS motifs, was partly colocalized with HA-importin-α near or around the nuclear membrane, suggesting that NLS motif double mutants bind to importin-α but their binding efficiency is lower than that of wild-type core protein.

Finally, we examined the subcellular localization of core

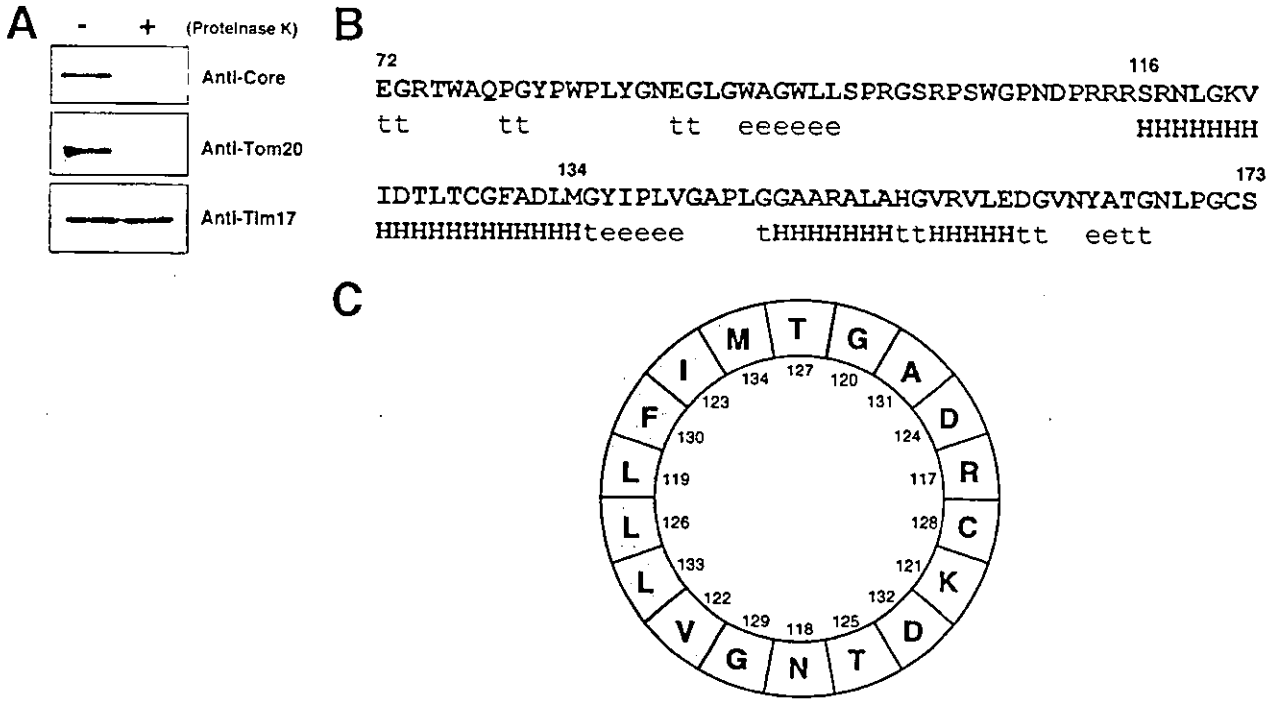

FIG. 6. (A) Protease protection assay. A mitochondrial fraction isolated from cells expressing the core protein was treated with proteinase K (+) as described in Materials and methods. The sample as well as the nontreated fraction (−) were subjected to immunoblotting with a monoclonal antibody against either HCV core, Tom20, or Tim17. (B) Protein sequence and predicted secondary structure of HCV core, amino acids 72 to 173. The secondary structure prediction was obtained with the self-optimized prediction method, a computer program on the internet (http://npsa-pbil.ibcp.fr/cgi-bin/npsa_automat.pl?page = /NPSA/npsa_sopm.html). H, α-helix; t, turn; e, extension. (C) α-Helical plot of amino acids 117 to 134 of the core protein. In the helical wheel plots, the gray shading represents apolar and hydrophobic residues; and the white represents polar residues.

protein expressed by the wild-type and NLS mutants (Fig. 7D). As expected, a fusion protein containing wild-type core protein (amino acids 1 to 71) and GFP was localized exclusively to the nucleus. Core proteins from three fusion proteins containing substitutions in each NLS motif (NLS/m1, NLS/m2, and NLS/m3) were detected primarily in the nucleus. Weak fluorescence was also observed in the cytoplasm, suggesting that these mutations caused a slight reduction in the efficiency of nuclear translocation. On the other hand, two or three NLS motif substitution mutations (NLS/m4, NLS/m5, NLS/m6, and NLS/m7) completely abolished nuclear translocation, resulting in a diffuse distribution of core protein, similar to that of GFP alone. Although it is likely that all three putative NLS motifs play a role, the above results suggest that at least two of the three putative NLS motifs are prerequisite for efficient nuclear translocation of the core protein.

DISCUSSION

HCV core protein is released from the viral polyprotein by a host protease(s) within the ER membrane at a signal peptide sequence lying between the core and envelope (E1) proteins (16, 41). Subsequently, the signal peptide is further processed by an intramembranous protease called signal peptide peptidase (38, 53). This mature form of the core protein is then released and undergoes subcellular trafficking (30, 53). The core protein localizes mainly to the ER, mitochondria, and lipid droplets. Some reports also describe localization of the core protein to the nuclei of hepatocytes in HCV-infected patients (10), transgenic mice (34), and cultured cells expressing viral polyproteins (56). Although it has been reported which sequence motifs are responsible for localization of the HCV core protein to lipid droplets and nuclei, it is uncertain which sequences target the core protein to the ER and to mitochondria. In this study, we identified sequences related to localization of the mature core protein to the ER and to mitochondria.

Through heterologous expression of core-GFP fusion proteins containing a series of deletions, we determined that a sequence extending from amino acids 112 to 152 of the core protein is required for its localization at the mitochondrial outer membrane. Translocation of nucleus-encoded mitochondrial proteins is usually dependent on N-terminal sequences, referred to as mitochondrial targeting sequences (37). However, it is also true that a significant proportion of mitochondrial proteins lack these N-terminal mitochondrial targeting sequences. Specifically, a number of outer membrane proteins do not have cleavable sequences at their N termini; rather, they are targeted to mitochondria by means of internal or C-terminal signals (31).

Since it has been reported that amino acid sequences required for targeting to the outer mitochondrial membrane form a highly hydrophobic α-helical wheel, as seen in A-kinase associated protein 84/12 (4) and NADH-cytochrome *b* reduc-

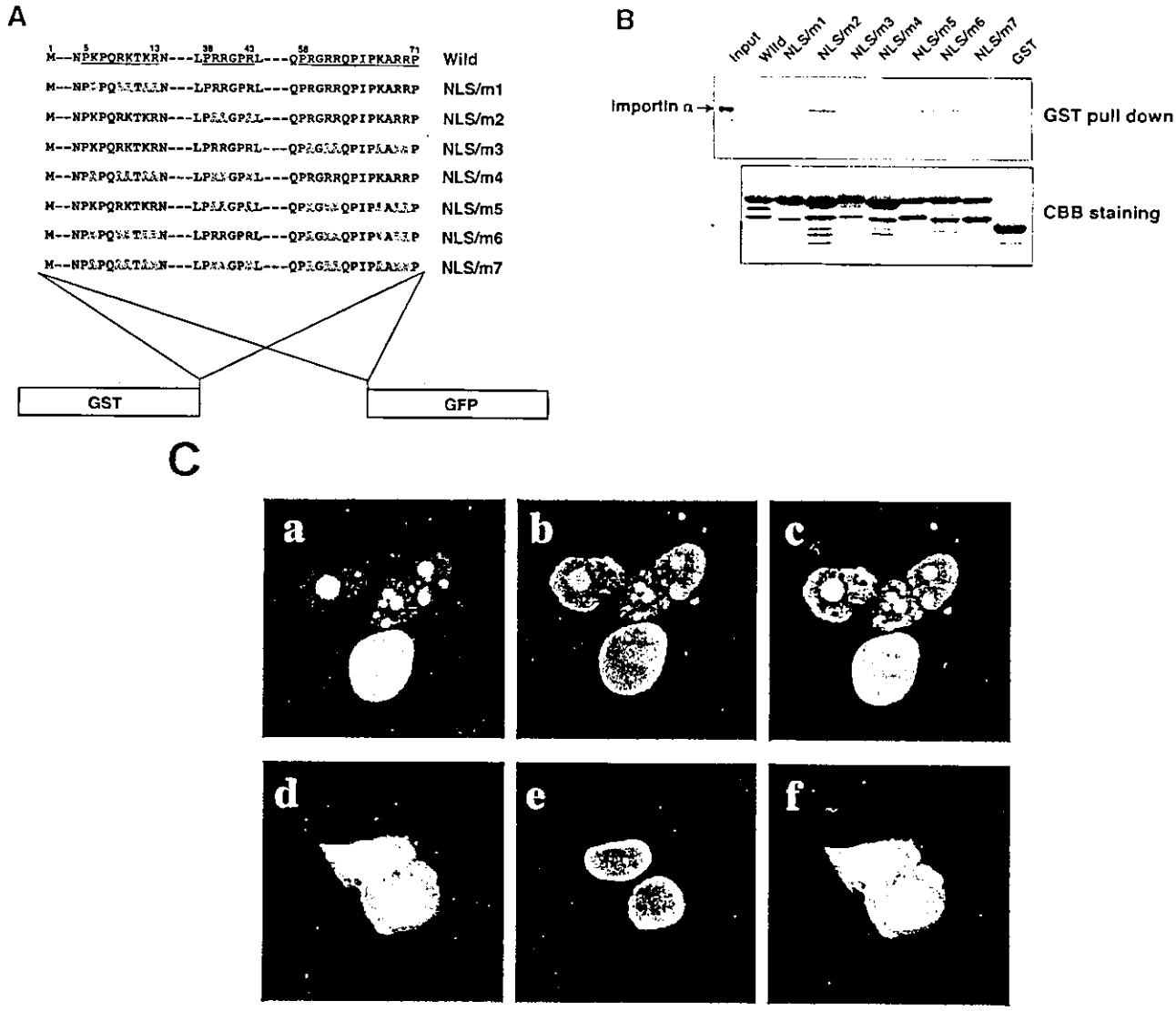

FIG. 7. Mutational analyses of NLS motifs in HCV core protein. (A) Schematic structures of fusion proteins and amino acid sequences corresponding to putative NLS motifs, three basic clusters (underlined) in the core protein. Two series of constructs fused with either GFP or GST were created. The mutated basic residues are indicated with outline letters. (B) GST pulldown assay. Equal amounts of GST fusions as described in A or GST alone was immobilized on glutathione-Sepharose 4B beads and incubated with in vitro-translated, [^{35}S]methionine-labeled importin-α. Bound material was separated by SDS-PAGE, and the amount of importin-α bound was detected by autoradiography. Direct electrophoretic separation of in vitro translation products served as a control (input). Coomassie brilliant blue staining of GST fusions and GST alone are shown in the bottom panel. (C) Confocal analysis of double staining for core-GFP fusion protein and HA-importin-α. 293T cells transfected with the wild-type core (1–71)-GFP (a to c) or NLS/m4 (d to f) expression plasmid and pCAG-HA-imp were allowed to express for 2 days. After the cells were fixed and permeabilized, they were incubated with a mouse anti-HA antibody. The red signals corresponding to HA-importin-α were obtained with a rhodamine-conjugated goat anti-mouse IgG secondary antibody (b and e). Overlay resulted in yellow signals indicative of colocalization (c and f). (D) Subcellular localization of GFP fusion proteins. GFP fusions with and without substitution mutations in the NLS motifs of the core protein as described in A were expressed in 293T cells. GFP images of the fixed cells were recorded.

tase (14), a predicted structure of an amphipathic α-helix present between amino acids 116 and 134 (Fig. 6B and C) possibly plays a role in directing the core protein to the mitochondrial outer membrane. Sequence comparisons demonstrate conservation of the amino acid sequence and secondary structure of the region, amino acids 112 to 152, among a variety of HCV isolates, including the infectious H77c clone (55), as well as a full-length adaptive replicon (3). To gain insight into the significance of the secondary structure of the region in targeting to the mitochondria, further structural and biochemical analyses are needed.

The association of HCV core protein with the mitochondrial membrane suggests that the core protein has the ability to modulate mitochondrial function, possibly by altering the permeability of the mitochondrial membrane. The core protein induces the production of cellular reactive oxygen species in

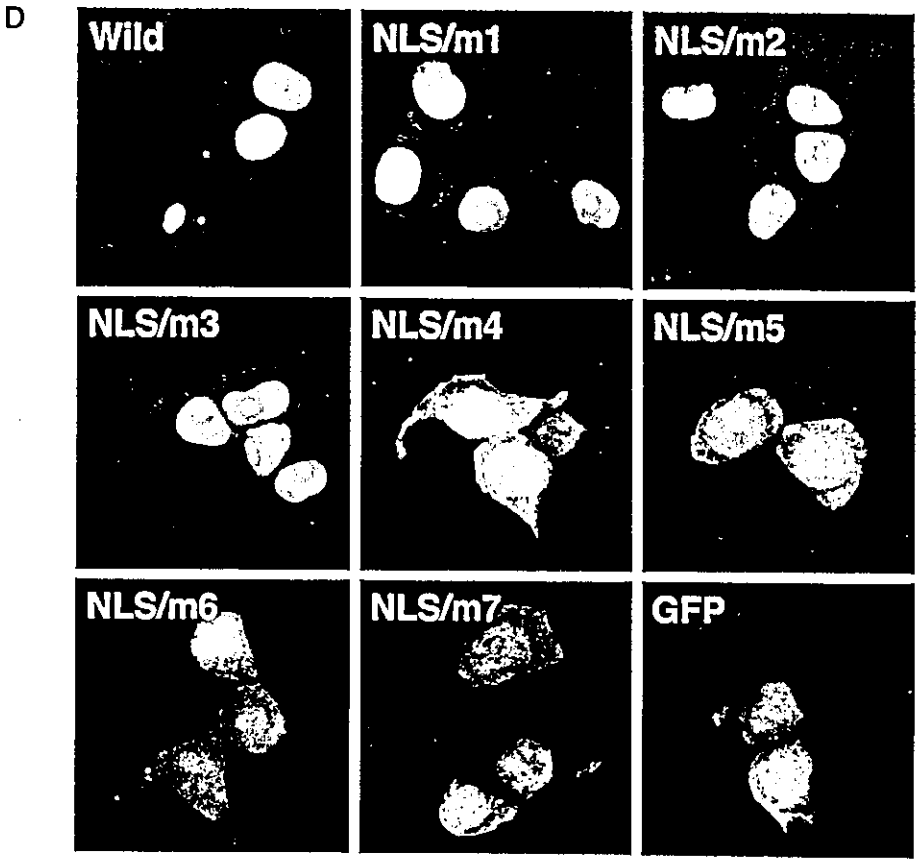

FIG. 7—*Continued.*

the livers of core-transgenic mice and in core-expressing cell lines (35). Reactive oxygen species, predominantly generated in mitochondria, induce genetic mutations and act as secondary messengers to regulate a variety of cellular functions, including gene expression and proliferation (1). Although the molecular mechanism by which core protein induces reactive oxygen species production is still unclear, HCV core protein is known to impair the mitochondrial electron transfer system (35). The core protein may also modulate apoptosis, since mitochondria play a major role in regulating programmed cell death. Expression of HCV proteins, including the core protein, suppresses the release of cytochrome *c* from mitochondria to the cytoplasm in HCV-transgenic mice, thus inhibiting Fas-mediated apoptosis (27).

Okamoto et al. recently reported that not only the C-terminal signal sequence but also amino acids 128 to 151 are required for ER retention of the core protein by using a series of N-terminally truncated core protein constructs (38). Here, in this study, we further showed that amino acids 112 to 152 mediate association of the core protein with the ER in the absence of the C-terminal signal sequence. Hope and McLauchlan demonstrated that the central domain of the core protein, amino acids 119 to 174, is important for association with lipid droplets (17). They also showed that this corresponding domain is shared with GB virus B, which is most closely related to HCV, but not with either pestiviruses or flaviviruses (18). It appears that the 41 residues identified as the sequence mediating association with the ER membrane in the present study are crucial for directing the core protein to lipid droplets, since the surface of lipid droplets must derive from the cytoplasmic side of the ER membrane.

The HCV core protein contains NLS sequences which are composed of three stretches of sequences rich in basic residues. These sequences were originally identified by experiments with fused forms of wild-type and mutated core proteins with β-galactosidase (6, 48). C-terminally truncated versions of the core protein localize exclusively to the nucleus (48). A fraction of the core protein is detected in the nucleus even when full-length HCV core gene is expressed (Fig. 2) and as described (34, 56). However, it is difficult to demonstrate clearly the nuclear localization of the core protein by immunofluorescence, presumably because of the instability of nuclearly localized core protein (49, 33). We only observed a nuclear staining pattern of the matured core protein after adding proteasome inhibitors to the culture (33).

Generally, NLS sequences fall into two categories: (i) monopartite NLSs, which contain a single cluster of basic residues, and (ii) bipartite NLSs, which contain two clusters of basic residues separated by an unconserved linker sequence of variable length (reviewed in reference 12). Nuclear translocation of an NLS-containing cargo protein is initiated when the soluble import receptor (importin) recognizes the NLS-contain-

ing protein within the cytoplasm. Importin-α contains an NLS-binding site(s), and importin-β docks importin-cargo complexes to the cytoplasmic filaments of a nuclear pore complex, after which translocation occurs through the nuclear pore. Thus, importin-α functions as an adaptor between the bona fide import receptor and the NLS-containing protein.

We further characterized the NLS of the core protein and found that each of the NLS motifs of the core protein is able to bind to importin-α and that at least two NLS motifs are required for efficient nuclear distribution of the core protein in cells. It appears that double mutations among three NLS motifs decrease the ability of the core protein to bind importin-α. These observations suggest that the binding of the double mutants with importin-α leads to no or little active translocation of the core protein into the nucleus. The double mutations may also block subsequent interactions with importin-β1, GTPase Ran, and/or NTF2/p10, which are required for translocation through the nuclear pore complexes.

The findings obtained in this study suggest that HCV core protein NLS motifs have a bipartite function. Crystallographic studies of monopartite (e.g., simian virus 40 large T antigen) and bipartite (e.g., nucleoplasmin) NLSs show that the basic residue clusters of bipartite NLSs occupy separate binding sites on importin-α. In contrast, while monopartite NLSs can bind to the same sites as bipartate NLSs on importin-α, they mainly bind to the N-terminal binding site, which is referred to as the major binding site on importin-α (9, 11). A recent report describes an importin-α variant with a mutation in the major site which results in decreased ability to bind both monopartite and bipartite NLSs. Another variant with a mutation in the minor site exhibits decreased binding only to bipartite NLS-containing proteins, making importin-α nonfunctional in vivo (22). Thus, we favor a model in which the core protein bipartite NLS, composed of any two of the three basic clusters, occupies both major and minor binding sites on importin-α, resulting in efficient nuclear translocation. Importin-α may be equally accessible to all clusters, given their close proximity to one another, as well as the distinct conformational flexibility of the ≈70-residue N-terminal region of the core protein.

With regard to the molecular mechanisms participating in nuclear localization of the core protein, Moriishi et al. found that PA28γ is involved in nuclear localization of the core protein. Interaction of the core protein with PA28γ plays an important role in retention of the core protein in the nucleus (33). Furthermore, in yeast cells, nuclear transport of the core protein requires the activity of the small GTPase Ran/Gsp1p and is mediated by Kap123p, but neither importin-α nor importin-β is involved (20). Differences in nucleocytoplasmic transport between yeast and mammalian cells might explain the inconsistencies observed in the present study. Further experiments are required to characterize the exact nature of the interaction between the core protein and components of the nuclear import machinery, particularly in cells where HCV is replicating.

In conclusion, the mature HCV core protein has an internal 41-amino-acid sequence mediating association of the viral protein with the ER and mitochondria. We also provide evidence for a novel class of bipartite NLS contained within the core protein, which comprises two of three basic motifs, thus enabling efficient nuclear targeting. Multiple functional domains influence the subcellular localization of the core protein, which ultimately depends on the balance of the respective signals.

ACKNOWLEDGMENTS

We thank colleagues in the laboratories of the Department of Virology II at the National Institute of Infectious Diseases of Japan for providing advice and help. We especially thank Mami Matsuda and Makiko Yahata for assistance in sequencing and the preparation of experimental reagents and Tomoko Mizoguchi for secretarial work. We are grateful to Karsten Weis for providing us with the plasmid containing importin-α cDNA.

This work was supported in part by Second Term Comprehensive 10-Year Strategy for Cancer Control and Research on Emerging and Reemerging Infectious Diseases, Health Sciences Research Grants of the Ministry of Health, Labor and Welfare, and by the Program for Promotion of Fundamental Studies in Health Sciences of the Organization for Drug ADR Relief, R&D Promotion and Product Review of Japan (JD:01–3). This work was also supported in part by a Grant-in-Aid for Young Scientists from the Ministry of Education, Culture, Sports, Science and Technology to R.S. (15790244).

REFERENCES

1. **Adler, V., Z. Yin, K. D. Tew, and Z. Ronai.** 1999. Role of redox potential and reactive oxygen species in stress signaling. Oncogene 18:6104–6111.
2. **Barba, G., F. Harper, T. Harada, M. Kohara, S. Goulinet, Y. Matsuura, G. Eder, Z. Schaff, M. J. Chapman, T. Miyamura, and C. Bréchot.** 1997. Hepatitis C virus core protein shows a cytoplasmic localization and associates to cellular lipid storage droplets. Proc. Natl. Acad. Sci. USA 94:1200–1205.
3. **Bukh, J., T. Pietschmann, V. Lohmann, N. Krieger, K. Faulk, R. E. Engle, S. Govindarajan, M. Shapiro, M. St Claire, and R. Bartenschlager.** 2002. Mutations that permit efficient replication of hepatitis C virus RNA in Huh-7 cells prevent productive replication in chimpanzees. Proc. Natl. Acad. Sci. USA 99:14416–14421.
4. **Cardone, L., T. de Cristofaro, A. Affaitati, C. Garbi, M. D. Ginsberg, M. Saviano, S. Varrone, C. S. Rubin, M. E. Gottesman, E. V. Avvedimento, and A. Feliciello.** 2002. A-kinase anchor protein 84/121 are targeted to mitochondria and mitotic spindles by overlapping amino-terminal motifs. J. Mol. Biol. 320:663–675.
5. **Chang, J., S. H. Yang, Y. G. Cho, S. B. Hwang, Y. S. Hahn, and Y. C. Sung.** 1998. Hepatitis C virus core from two different genotypes has an oncogenic potential but is not sufficient for transforming primary rat embryo fibroblasts in cooperation with the H-ras oncogene. J. Virol. 72:3060–3065.
6. **Chang, S. C., J. H. Yen, H. Y. Kang, M. H. Jang, and M. F. Chang.** 1994. Nuclear localization signals in the core protein of hepatitis C virus. Biochem. Biophys. Res. Commun. 205:1284–1290.
7. **Choo, Q. L., G. Kuo, A. J. Weiner, L. R. Overby, D. W. Bradley, and M. Houghton.** 1989. Isolation of a cDNA clone derived from a blood-borne non-A, non-B viral hepatitis genome. Science 244:359–362.
8. **Choo, Q. L., K. H. Richman, J. H. Han, K. Berger, C. Lee, C. Dong, C. Gallegos, D. Coit, R. Medina-Selby, P. J. Barr, et al.** 1991. Genetic organization and diversity of the hepatitis C virus. Proc. Natl. Acad. Sci. USA 88:2451–2455.
9. **Conti, E., M. Uy, L. Leighton, G. Blobel, and J. Kuriyan.** 1998. Crystallographic analysis of the recognition of a nuclear localization signal by the nuclear import factor karyopherin alpha. Cell 94:193–204.
10. **Falcon, V., N. Acosta-Rivero, G. Chinea, M. C. de la Rosa, I. Menendez, S. Duenas-Carrera, B. Gra, A. Rodriguez, V. Tsutsumi, M. Shibayama, J. Luna-Munoz, M. M. Miranda-Sanchez, J. Morales-Grillo, and J. Kouri.** 2003. Nuclear localization of nucleocapsid-like particles and HCV core protein in hepatocytes of a chronically HCV-infected patient. Biochem. Biophys. Res. Commun. 310:54–58.
11. **Fontes, M. R., T. Teh, and B. Kobe.** 2000. Structural basis of recognition of monopartite and bipartite nuclear localization sequences by mammalian importin-alpha. J. Mol. Biol. 297:1183–1194.
12. **Görlich, D., and U. Kutay.** 1999. Transport between the cell nucleus and the cytoplasm. Annu. Rev. Cell. Dev. Biol. 15:607–660.
13. **Grakoui, A., D. W. McCourt, C. Wychowski, S. M. Feinstone, and C. M. Rice.** 1993. Characterization of the hepatitis C virus-encoded serine proteinase: determination of proteinase-dependent polyprotein cleavage sites. J. Virol. 67:2832–2843.
14. **Hahne, K., V. Haucke, L. Ramage, and G. Schatz.** 1994. Incomplete arrest in the outer membrane sorts NADH-cytochrome b5 reductase to two different submitochondrial compartments. Cell 79:829–839.
15. **Harada, S., Y. Watanabe, K. Takeuchi, T. Suzuki, T. Katayama, Y. Takebe, I. Saito, and T. Miyamura.** 1991. Expression of processed core protein of hepatitis C virus in mammalian cells. J. Virol. 65:3015–3021.
16. **Hijikata, M., N. Kato, Y. Ootsuyama, M. Nakagawa, and K. Shimotohno.** 1991. Gene mapping of the putative structural region of the hepatitis C virus

genome by in vitro processing analysis. Proc. Natl. Acad. Sci. USA 88:5547–5551.
17. **Hope, R. G., and J. McLauchlan.** 2000. Sequence motifs required for lipid droplet association and protein stability are unique to the hepatitis C virus core protein. J. Gen. Virol. 81:1913–1925.
18. **Hope, R. G., D. J. Murphy, and J. McLauchlan.** 2002. The domains required to direct core proteins of hepatitis C virus and GB virus-B to lipid droplets share common features with plant oleosin proteins. J. Biol. Chem. 277:4261–4270.
19. **Hüssy, P., H. Langen, J. Mous, and H. Jacobsen.** 1996. Hepatitis C virus core protein: carboxy-terminal boundaries of two processed species suggest cleavage by a signal peptide peptidase. Virology 224:93–104.
20. **Isoyama, T., S. Kuge, and A. Nomoto.** 2002. The core protein of hepatitis C virus is imported into the nucleus by transport receptor Kap123p but inhibits Kap121p-dependent nuclear import of yeast AP1-like transcription factor in yeast cells. J. Biol. Chem. 277:39634–39641.
21. **Lai, M. M., and C. F. Ware.** 2000. Hepatitis C virus core protein: possible roles in viral pathogenesis. Curr. Top. Microbiol. Immunol. 242:117–134.
22. **Leung, S. W., M. T. Harreman, M. R. Hodel, A. E. Hodel, and A. H. Corbett.** 2003. Dissection of the karyopherin alpha nuclear localization signal (NLS)-binding groove: functional requirements for NLS binding. J. Biol. Chem. 278:41947–41953.
23. **Liu, Q., C. Tackney, R. A. Bhat, A. M. Prince, and P. Zhang.** 1997. Regulated processing of hepatitis C virus core protein is linked to subcellular localization. J. Virol. 71:657–662.
24. **Lo, S. Y., F. Masiarz, S. B. Hwang, M. M. Lai, and J. H. Ou.** 1995. Differential subcellular localization of hepatitis C virus core gene products. Virology 213:455–461.
25. **Lo, S. Y., M. Selby, M. Tong, and J. H. Ou.** 1994. Comparative studies of the core gene products of two different hepatitis C virus isolates: two alternative forms determined by a single amino acid substitution. Virology 199:124–131.
26. **Lu, W., A. Strohecker, and J. H. Ou.** 2001. Post-translational modification of the hepatitis C virus core protein by tissue transglutaminase. J. Biol. Chem. 276:47993–47999.
27. **Machida, K., K. Tsukiyama-Kohara, E. Seike, S. Tone, F. Shibasaki, M. Shimizu, H. Takahashi, Y. Hayashi, N. Funata, C. Taya, H. Yonekawa, and M. Kohara.** 2001. Inhibition of cytochrome c release in Fas-mediated signaling pathway in transgenic mice induced to express hepatitis C viral proteins. J. Biol. Chem. 276:12140–12146.
28. **Matsumoto, M., S. B. Hwang, K. S. Jeng, N. Zhu, and M. M. Lai.** 1996. Homotypic interaction and multimerization of hepatitis C virus core protein. Virology 218:43–51.
29. **McLauchlan, J.** 2000. Properties of the hepatitis C virus core protein: a structural protein that modulates cellular processes. J. Viral Hepatitis 7:2–14.
30. **McLauchlan, J., M. K. Lemberg, G. Hope, and B. Martoglio.** 2002. Intramembrane proteolysis promotes trafficking of hepatitis C virus core protein to lipid droplets. EMBO J. 21:3980–3988.
31. **Mihara, K.** 2000. Targeting and insertion of nuclear-encoded preproteins into the mitochondrial outer membrane. Bioessays 22:364–371.
32. **Moradpour, D., C. Englert, T. Wakita, and J. R. Wands.** 1996. Characterization of cell lines allowing tightly regulated expression of hepatitis C virus core protein. Virology 222:51–63.
33. **Moriishi, K., T. Okabayashi, K. Nakai, K. Moriya, K. Koike, S. Murata, T. Chiba, K. Tanaka, R. Suzuki, T. Suzuki, T. Miyamura, and Y. Matsuura.** 2003. Proteasome activator PA28gamma-dependent nuclear retention and degradation of hepatitis C virus core protein. J. Virol. 77:10237–10249.
34. **Moriya, K., H. Fujie, Y. Shintani, H. Yotsuyanagi, T. Tsutsumi, K. Ishibashi, Y. Matsuura, S. Kimura, T. Miyamura, and K. Koike.** 1998. The core protein of hepatitis C virus induces hepatocellular carcinoma in transgenic mice. Nat. Med. 4:1065–1067.
35. **Moriya, K., K. Nakagawa, T. Santa, Y. Shintani, H. Fujie, H. Miyoshi, T. Tsutsumi, T. Miyazawa, K. Ishibashi, T. Horie, K. Imai, T. Todoroki, S. Kimura, and K. Koike.** 2001. Oxidative stress in the absence of inflammation in a mouse model for hepatitis C virus-associated hepatocarcinogenesis. Cancer Res. 61:4365–4370.
36. **Moriya, K., H. Yotsuyanagi, Y. Shintani, H. Fujie, K. Ishibashi, Y. Matsuura, T. Miyamura, and K. Koike.** 1997. Hepatitis C virus core protein induces hepatic steatosis in transgenic mice. J. Gen. Virol. 78:1527–1531.
37. **Neupert, W.** 1997. Protein import into mitochondria. Annu. Rev. Biochem. 66:863–917.
38. **Okamoto, K., K. Moriishi, T. Miyamura, and Y. Matsuura.** 2004. Intramembrane proteolysis and endoplasmic reticulum retention of hepatitis C virus core protein. J. Virol. 78:6370–6380.
39. **Okuda, M., K. Li, M. R. Beard, L. A. Showalter, F. Scholle, S. M. Lemon, and S. A. Weinman.** 2002. Mitochondrial injury, oxidative stress, and antioxidant gene expression are induced by hepatitis C virus core protein. Gastroenterology 122:366–375.
40. **Perlemuter, G., A. Sabile, P. Letteron, G. Vona, A. Topilco, Y. Chretien, K. Koike, D. Pessayre, J. Chapman, G. Barba, and C. Bréchot.** 2002. Hepatitis C virus core protein inhibits microsomal triglyceride transfer protein activity and very low density lipoprotein secretion: a model of viral-related steatosis. FASEB J. 16:185–194.
41. **Ralston, R., K. Thudium, K. Berger, C. Kuo, B. Gervase, J. Hall, M. Selby, G. Kuo, M. Houghton, and Q. L. Choo.** 1993. Characterization of hepatitis C virus envelope glycoprotein complexes expressed by recombinant vaccinia viruses. J. Virol. 67:6753–6761.
42. **Ray, R. B., L. M. Lagging, K. Meyer, and R. Ray.** 1996. Hepatitis C virus core protein cooperates with ras and transforms primary rat embryo fibroblasts to tumorigenic phenotype. J. Virol. 70:4438–4443.
43. **Roth, J., D. J. Taatjes, and M. J. Warhol.** 1989. Prevention of non-specific interactions of gold-labeled reagents on tissue sections. Histochemistry 92:47–56.
44. **Sabile, A., G. Perlemuter, F. Bono, K. Kohara, F. Demaugre, M. Kohara, Y. Matsuura, T. Miyamura, C. Brechot, and G. Barba.** 1999. Hepatitis C virus core protein binds to apolipoprotein AII and its secretion is modulated by fibrates. Hepatology 30:1064–1076.
45. **Santolini, E., G. Migliaccio, and N. La Monica.** 1994. Biosynthesis and biochemical properties of the hepatitis C virus core protein. J. Virol. 68:3631–3641.
46. **Selby, M. J., Q. L. Choo, K. Berger, G. Kuo, E. Glazer, M. Eckart, C. Lee, D. Chien, C. Kuo, and M. Houghton.** 1993. Expression, identification and subcellular localization of the proteins encoded by the hepatitis C viral genome. J. Gen. Virol. 74:1103–1113.
47. **Shimoike, T., S. Mimori, H. Tani, Y. Matsuura, and T. Miyamura.** 1999. Interaction of hepatitis C virus core protein with viral sense RNA and suppression of its translation. J. Virol. 73:9718–9725.
48. **Suzuki, R., Y. Matsuura, T. Suzuki, A. Ando, J. Chiba, S. Harada, I. Saito, and T. Miyamura.** 1995. Nuclear localization of the truncated hepatitis C virus core protein with its hydrophobic C terminus deleted. J. Gen. Virol. 76:53–61.
49. **Suzuki, R., K. Tamura, J. Li, K. Ishii, Y. Matsuura, T. Miyamura, and T. Suzuki.** 2001. Ubiquitin-mediated degradation of hepatitis C virus core protein is regulated by processing at its carboxyl terminus. Virology 280:301–309.
50. **Tanaka, Y., T. Shimoike, K. Ishii, R. Suzuki, T. Suzuki, H. Ushijima, Y. Matsuura, and T. Miyamura.** 2000. Selective binding of hepatitis C virus core protein to synthetic oligonucleotides corresponding to the 5′ untranslated region of the viral genome. Virology 270:229–236.
51. **Tellinghuisen, T. L., and C. M. Rice.** 2002. Interaction between hepatitis C virus proteins and host cell factors. Curr. Opin. Microbiol. 5:419–427.
52. **Thomson, M., and T. J. Liang.** 2000. Molecular biology of hepatitis C virus, p. 1–23. *In* T. J. Liang and J. H. Hoofnagle (ed.), Hepatitis C. Academic Press, San Diego, Calif.
53. **Weihofen, A., K. Binns, M. K. Lemberg, K. Ashman, and B. Martoglio.** 2002. Identification of signal peptide peptidase, a presenilin-type aspartic protease. Science 296:2215–2218.
54. **Weis, K., I. W. Mattaj, and A. I. Lamond.** 1995. Identification of hSRP1 alpha as a functional receptor for nuclear localization sequences. Science 268:1049–1053.
55. **Yanagi, M., R. H. Purcell, S. U. Emerson, and J. Bukh.** 1997. Transcripts from a single full-length cDNA clone of hepatitis C virus are infectious when directly transfected into the liver of a chimpanzee. Proc. Natl. Acad. Sci. USA 94:8738–8743.
56. **Yasui, K., T. Wakita, K. Tsukiyama-Kohara, S. I. Funahashi, M. Ichikawa, T. Kajita, D. Moradpour, J. R. Wands, and M. Kohara.** 1998. The native form and maturation process of hepatitis C virus core protein. J. Virol. 72:6048–6055.

Arch Virol (2004) 149: 61–74
DOI 10.1007/s00705-003-0202-x

Archives of Virology
Printed in Austria

Cell cycle perturbation in a human hepatoblastoma cell line constitutively expressing *Hepatitis C virus* core protein

A. Ruggieri[1], M. Murdolo[1], T. Harada[2,3], T. Miyamura[2], and M. Rapicetta[1]

[1]Laboratory of Virology, Istituto Superiore di Sanità, Rome, Italy
[2]Department of Virology II, National Institute of Infectious Diseases, Tokyo, Japan
[3]Department of Immunology, IRIS Chiron S.p.A., Siena, Italy

Received January 9, 2003; accepted July 11, 2003
Published online September 22, 2003

Summary. *Hepatitis C virus* (HCV) is one of the major causes of chronic liver disease with the potential for development of hepatocellular carcinoma (HCC). The core protein of HCV has been shown to modulate expression of various cellular genes and to influence a number of cellular functions. We investigated the effect of constitutively expressed HCV core protein on cell cycle progression in HepG2 cell line, which is derived from a differentiated human hepatoblastoma and shows biosynthetic features similar to human hepatocytes. The results indicated that stable expression of the core protein in unsynchronized HepG2 cells induced a perturbation of the cell cycle with reduced cell doubling meantime and increased S phase fraction. Increase of *c-myc* protein above the basal expression level was demonstrated with a significant increase of *c-myc* stability, as revealed by its prolonged intracellular half-life, in HepG2 expressing HCV core protein. In contrast, p53 and p21 levels were unchanged. These results suggest that HCV core protein may promote cell cycle progression in HepG2 cells possibly through increasing stability of *c-myc* oncoprotein. These results are in support of important role played by HCV core protein in virus-mediated pathogenesis in persistently infected hosts and in hepatocarcinogenesis.

Introduction

Hepatitis C virus (HCV), a member of the family *Flaviviridae*, is the major cause of post-transfusion- and community-acquired viral hepatitis [6]. Persistent infection with HCV is a main cause of human liver disease and is strongly associated

with hepatocellular carcinoma [32]. In spite of increasing evidences about immunologically mediated and virus-induced mechanisms, so far pathogenic and carcinogenic processes associated to HCV infection are only partially understood [4].

HCV RNA genome is approximately 9.5 kb and encodes a single polyprotein of about 3000 amino acids [15]. This precursor protein is cleaved by the host- and viral proteases to generate three structural proteins at the N-terminal end and six nonstructural proteins at the C-terminal end [13, 15, 26]. The HCV core protein, with an apparent molecular mass of 21 kDa, is highly conserved among various HCV genotypes and it includes 191 amino acids at the N-terminal of the virus genome. In addition to its structural function in viral nucleocapsid formation, the core protein of HCV has been shown to be able to regulate expression of various host genes [17, 35] and to have roles in cell cycle acceleration [14] and in development of carcinoma through still not defined mechanisms [22]. Several studies indicated controversial effects of the core protein on apoptotic death, since it can promote apoptosis induced by Fas or TNF-α in stable expression systems in HepG2, HeLa and Jurkat T cell lines [11, 30, 39]. In contrast, transient expression of the core protein inhibited apoptosis induced by cisplatin in MCF7 cells [28], and by Fas or TNF-α [20]. From our previous studies a pro-apoptotic effect of the core protein toward anti-Fas mediated apoptosis has been shown in a human hepatoblastoma cell line constitutively expressing the core protein [31].

Some intracellular pathways including genes which are known to control cell growth and death, such as *c-myc*, p53 and p21, have been recognized to regulate cell cycle as well [16]. Regulation of cell cycle and apoptosis is essential to maintain cellular physiological conditions. In fact, impaired regulation of the cell cycle and especially the failure at G1/S or G2/M checkpoints is responsible for accumulation of detrimental mutations that may result in cell transformation. Furthermore a commitment state to apoptotic cell death may be induced [25, 33].

Viruses have evolved strategies to modulate cell cycle, influencing different checkpoints according to their requirement for replication and/or latency. Among RNA viruses, HTLV-1 stimulates cell proliferation and cell cycle progression from G0/G1 phase to S and G2/M phases in one of the T cell lines *in vitro* [24]. HIV *vpr* protein is also reported to alter cell cycle progression from G2 phase [36].

In the case of viral hepatitis, several *in vivo* studies on hepatic biopsies reported an imbalance between G1 and S phases in liver cells obtained from chronic hepatitis C patients [38]. Analysis to identify HCV gene product(s) responsible for the imbalance of cell cycle regulation so far has suggested a role of HCV core protein in accelerating entering the S phase in CHO cells *in vitro* [14]; in addition, up-regulation of cyclin E expression and cell proliferation by the core protein have been observed in Rat-1 cell lines [5].

Cell cycle progression and apoptosis are balanced processes regulated by a number of cellular factors variously expressed in cultured cells; perturbation of the cell cycle introduced by viral gene products in cell systems *in vitro* is conceivably related to specific targets for cell cycle activator or inhibitors which can be cell type specific [1]. However, previously reported observations about HCV core protein effect on cell cycle are all based upon *in vitro* systems in non-hepatic cell lines

of animal origin. Since HCV is a hepatotropic virus, it is more appropriate to use a hepatoblast cell line to study the effects of HCV core protein. Here we studied cell cycle progression and expression of some endogenous cell cycle regulators (p53, p21, *c-myc*) in hepatic cell line of human origin (HepG2 cells) constitutively expressing HCV core or other HCV structural proteins to examine the role of HCV core protein in cell cycle regulation.

Materials and methods

Cell lines, plasmids and reagents

Several clones from the human hepatoblastoma HepG2 cell line constitutively expressing HCV core (Hep39) protein were established by transfection with the plasmid pcEF39neo in which the cDNA coding for HCV core protein (aminoacid positions 1–194) was under the control of the EF1-α promoter; HepG2 cells expressing HCV E1-E2 proteins (Hep827) were obtained by transfecting cells with the plasmid pcEF827 carrying the HCV coding region corresponding to amino acid positions 155–810. Cells were also transfected with the expression vector pcEF321swxneo as a negative control (Hepswx) [12, 31]. Transfections were performed by calcium phosphate precipitation method. Transfectants HepG2 clones were grown in Dulbecco's Modified Eagle Medium (DMEM) supplemented with 10% FBS and 0.6 mg/ml of G418.

Anti-human *c-myc* monoclonal antibody (clone 9E10) was purchased from Santa Cruz, CA, USA; anti-p-53 (DO-7 clone) and anti-$p21^{WAF/CIP1}$ (SX118 clone) monoclonal antibodies were purchased from Pharmingen; anti β-actin monoclonal antibody was purchased from Sigma-Aldrich, Italy; anti-HCV core monoclonal antibody was provided by Dr. Yoshiharu Matsuura (Osaka University, Japan). Cyclohexamide was purchased from Sigma (Sigma-Aldrich, Italy) and concentration of the stock solution was 5 mg/ml.

Cell growth and proliferation assays

Cell growth assay was performed according to standard methods [9]. For cell growth analysis, 1×10^5 cells were seeded onto six wells plates in duplicate at day 0. Cells were daily trypsinized and live cells were counted with trypan blue. Duplicate wells were counted at each time point and the population doubling time was obtained from day 1 to day 4.

Hep39 cell proliferation was assessed by MTT assay. Ten thousands cells were seeded per well in 96-wells plates and analysed after 24 and 72 h using a Cell Proliferation kit I (MTT Roche Diagnostics) according to the manufacturer's instructions.

Cell cycle analysis

The cell cycle phase distribution in each cell population was determined by measuring the DNA content of individual cell line by flow cytometry. For this purpose cells were trypsinized, pelleted by centrifugation and approximately 10^6 cells were resuspended in citrate buffer (250 mmol/L sucrose, 40 mmol/L trisodium citrate and 20% dimethyl sulfoxyde), followed by incubation for 10 min at room temperature with a 0.03% trypsin solution containing 3.4 mmol/L trisodium citrate, 1.5 mmol/L spermine, 0.5 mmol/L Tris and 0.01% Nonidet P-40 (pH 7.6). Samples were incubated for additional 10 min after the addition of trypsin inhibitor (0.5 mg/ml) and ribonuclease A (0.1 mg/ml) and then stained by propidium iodide (0.4 mg/ml) for 10 min at room temperature. The samples were analysed by a FACScalibur (Becton Dickinson) flow cytometer using Cell Quest software. Cell cycle phase distributions were quantified using ModFit LT version 3.0 software.